COLLÈGE DE FRANCE
1530

Chaire de Physique de la Matière Condensée

Cuprates supraconducteurs : où en est-on ?

Antoine Georges

Cycle 2010-2011
Cours 2&3 – 9&16/11/2010

Cours 3 - 16/11/2010

Cours: Phénoménologie des cuprates supraconducteurs (suite) :

pseudogap, dichotomie nœuds/antinœuds

- 15h30: Christophe BERTHOD, Université de Genève, *Spectroscopie STM dans les cuprates*
- 16h45: Kamran BEHNIA, ESPCI, *Transport d'entropie dans les cuprates supraconducteurs*

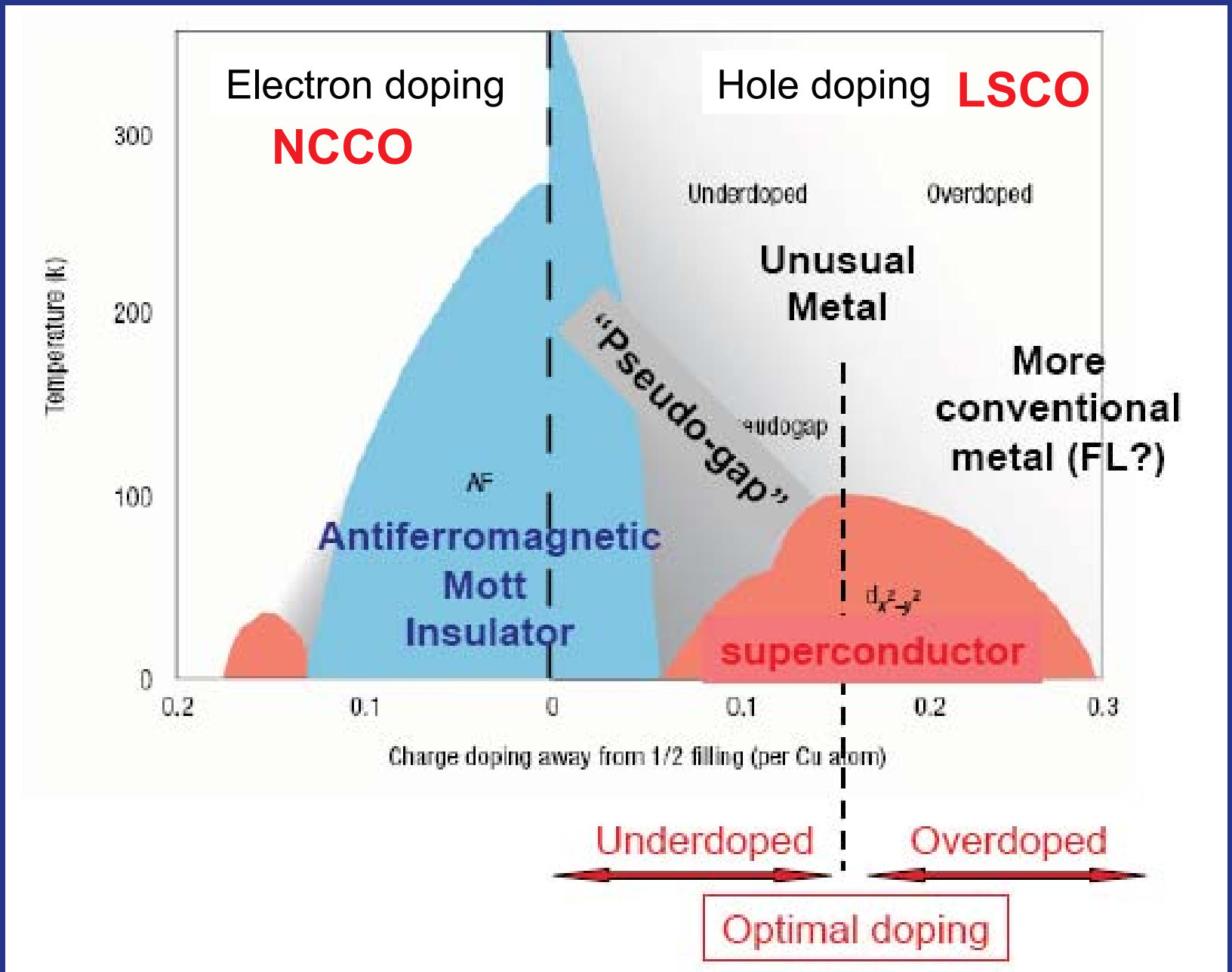

Cuprates: “Generic” phase diagram

Different materials must be considered to explore the whole phase diagram… the example of ARPES

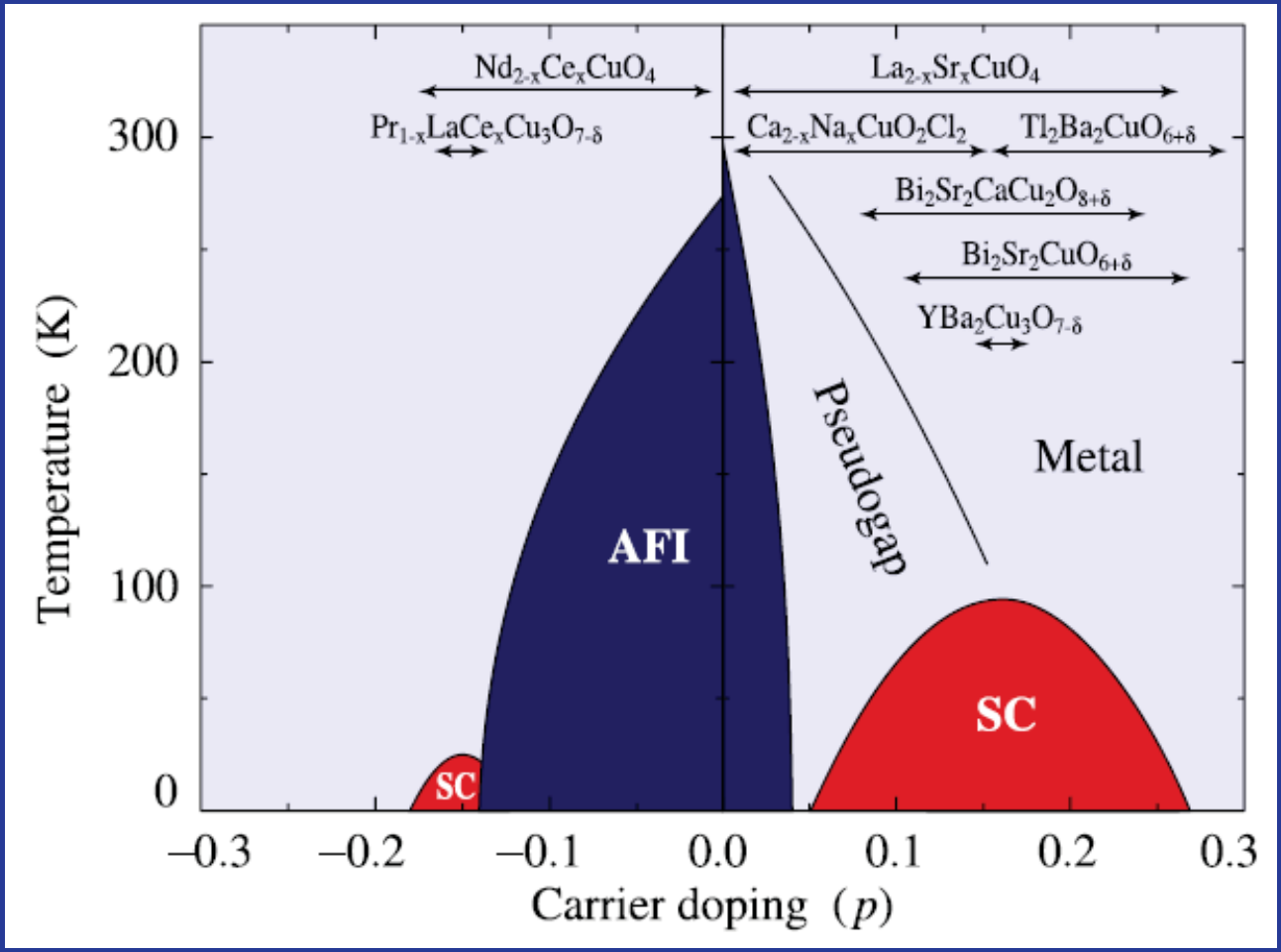

From: Peets et al. New J. Phys (2006)

1. Parent compounds: Antiferromagnetic Insulators

LSCO: T_N ~ 325 K

$YBCO_6$ T_N ~ 500 K

NCCO (e-doped) T_N ~ 250 K

Fits to the spin-wave spectrum of La_2CuO_4

* Early (1989-1991) neutron experiments compared to theoretical spin-wave spectra yielded estimates of the intra-plane nearest neighbor exchange

J ~ 116-136 meV ~ 1400 – 1550 K

(and weak inter-plane exchange ~ 0.002 meV)

Ordered moment: 0.6 μ_B (Free Cu^{2+}: 1.1μ_B) → Importance of quantum fluctuations

* More recent high-precision neutron experiments point, additionally, at the importance of a 4-site exchange coupling cf. Coldea et al. PRL 86, 5377 (2001)

- This was anticipated from photon spectroscopies, e.g. Raman scattering (e.g. Sugai et al. PRB 42, 1045 (1990))

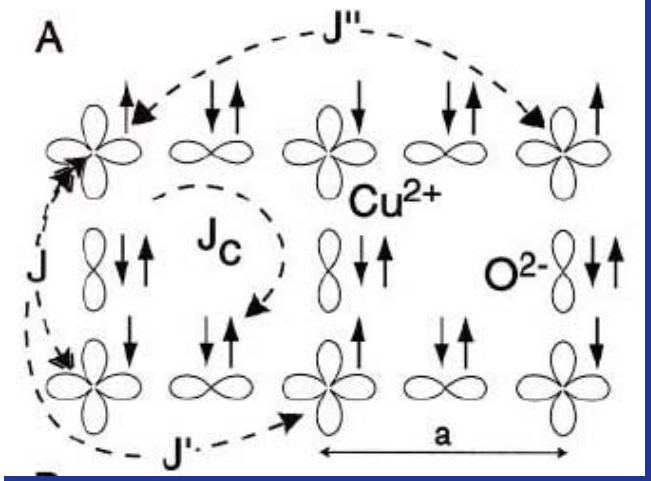

$$\mathcal{H} = J \sum_{\langle i,j \rangle} S_i \cdot S_j + J' \sum_{\langle i,i' \rangle} S_i \cdot S_{i'} + J'' \sum_{\langle i,i'' \rangle} S_i \cdot S_{i''} + J_c \sum_{\langle i,j,k,l \rangle} \{(S_i \cdot S_j)(S_k \cdot S_l) + (S_i \cdot S_l)(S_k \cdot S_j) - (S_i \cdot S_k)(S_j \cdot S_l)\}, \quad (1)$$

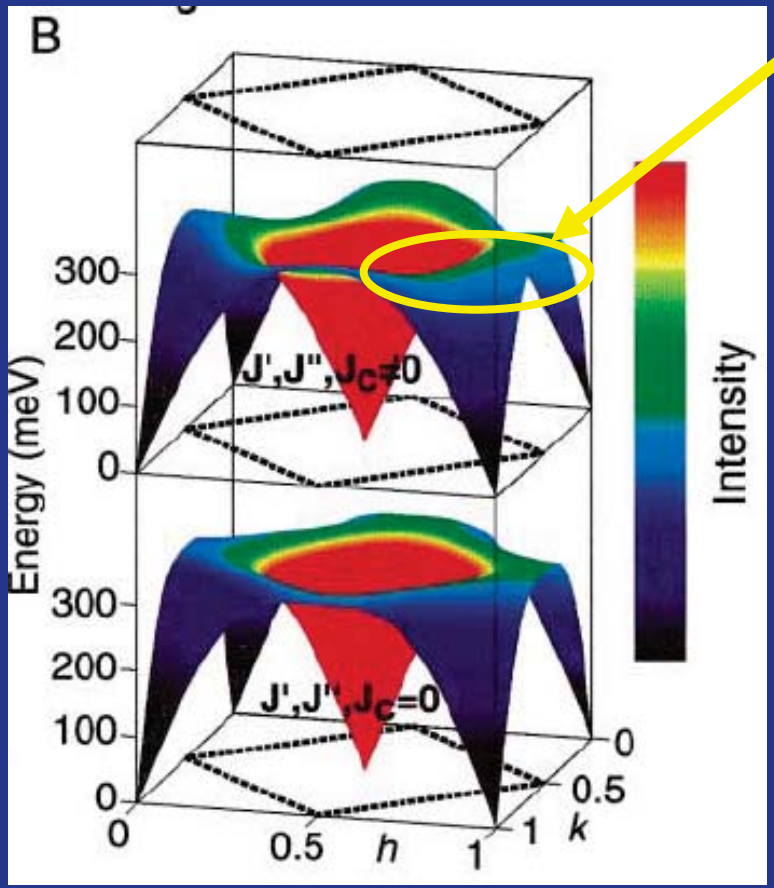

Weak variation of SW dispersion
Along the magnetic BZ boundary

Calculated SW
spectrum with
J = 138 meV, J'= J''= 2meV
J_c= 38(8) meV

Calculated SW
Spectrum with
n.n. J = 136 meV
only

Coldea et al.
2001

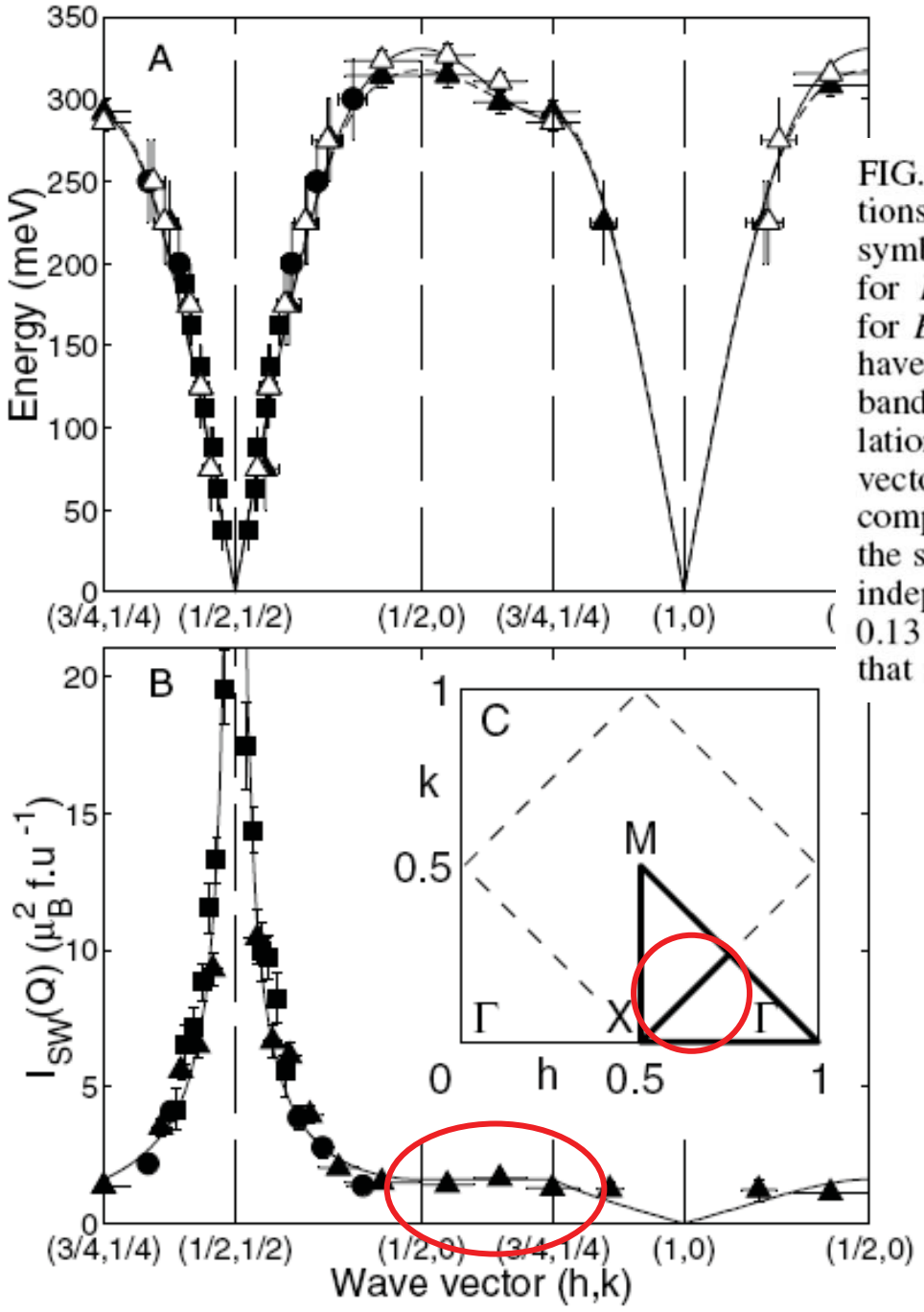

FIG. 3. (A) Dispersion relation along high symmetry directions in the 2D Brillouin zone, see inset (C), at $T = 10$ K (open symbols) and 295 K (solid symbols). Squares were obtained for $E_i = 250$ meV, circles for $E_i = 600$ meV, and triangles for $E_i = 750$ meV. Points extracted from constant-E(-Q) cuts have a vertical (horizontal) bar to indicate the $E(Q)$ integration band. Solid (dashed) line is a fit to the spin-wave dispersion relation at $T = 10$ K (295 K) as discussed in the text. (B) Wave-vector dependence of the spin-wave intensity at $T = 295$ K compared with predictions of linear spin-wave theory shown by the solid line. The absolute intensities [11] yield a wave-vector-independent intensity-lowering renormalization factor of 0.51 $\pm$ 0.13 in agreement with the theoretical prediction of 0.61 [12] that includes the effects of quantum fluctuations.

Please appreciate the accuracy of the theoretical vs. experimental comparison !

Reasonable agreement with estimates from 3-band p-d model

Perturbative estimate to lowest orders in t_{pd} :

$$J = \left(\frac{2t_{pd}^2}{\Delta}\right)^2 \left[\frac{1}{\Delta} + \frac{1}{U_{dd}}\right]$$

$$J^{(8)}_{\square,\mathrm{dir}} = \frac{80\, t_{pd}^8\, (U+\Delta_{pd})\, (U^2 + U\,\Delta_{pd} + \Delta_{pd}^2)}{U^3\, \Delta_{pd}^7}$$

With t_{pd}=1.3 eV, Δ = 3.6 eV, U=8 eV this would yield J ~ 350 meV, too large by a factor 2-3 !

But more precise estimates with cluster-cell method work much better,

Also for 4-spin exchange J_c:

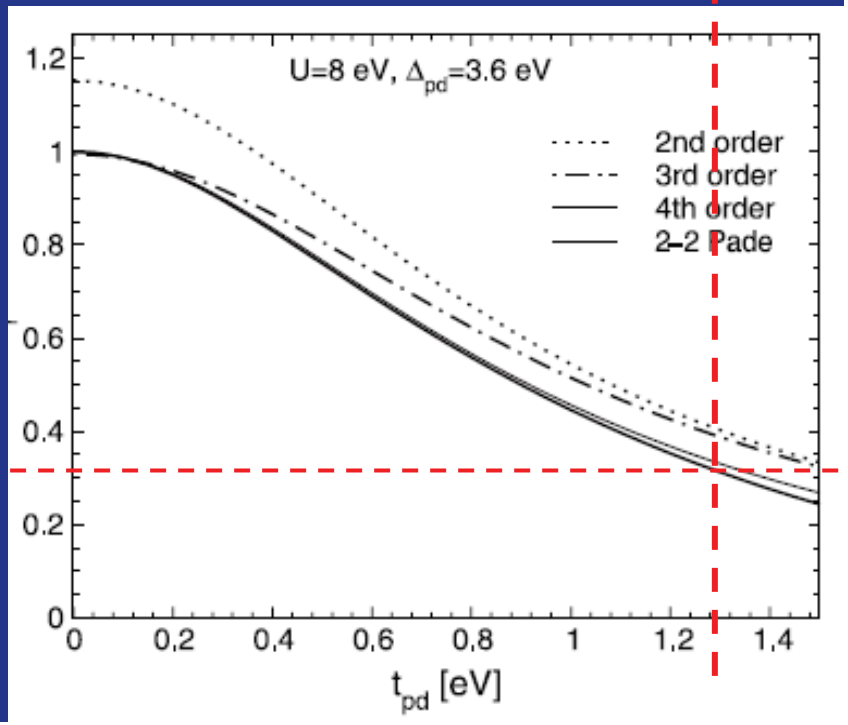

Muller-Hartmann and Reichl
EPJB 28, 173 (2002)

2. **Effect of doping on magnetism:**

- Destruction of long-range order
- Survival of magnetic correlations

Hole motion is detrimental to AF ordering… and AF ordering impedes the motion of holes

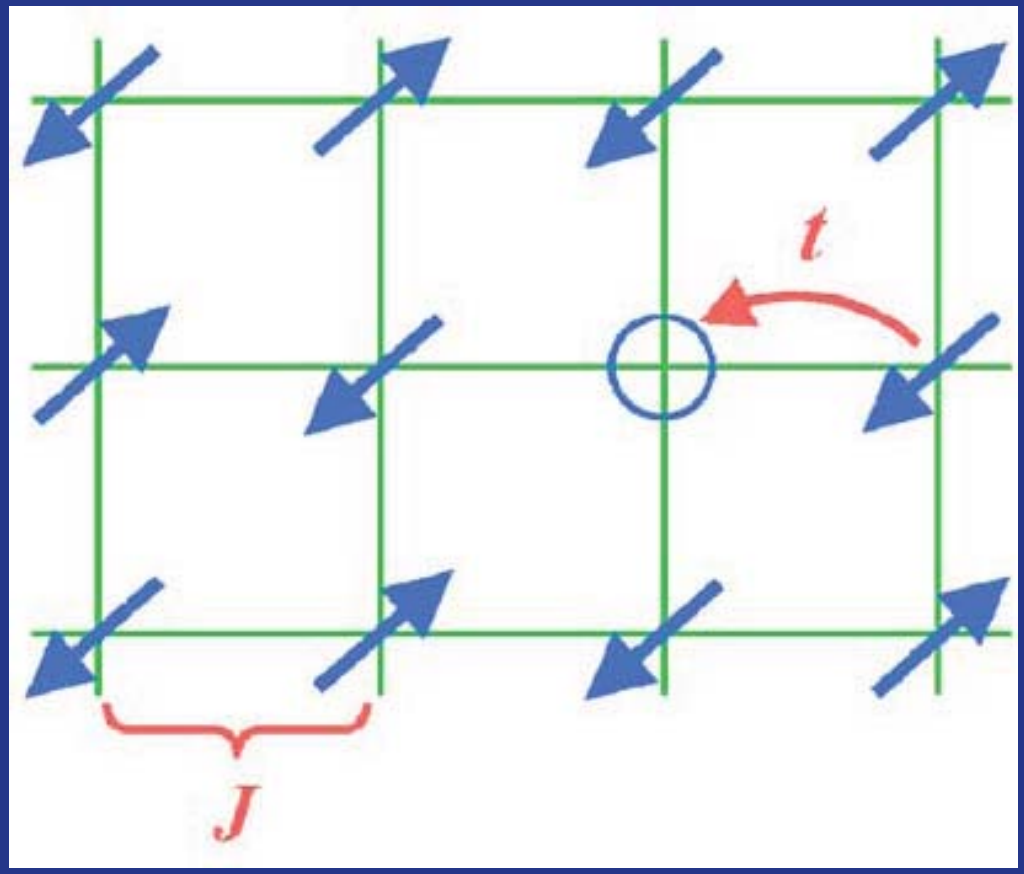

Note: Antiferromagnetism is more robust for electron-doped, see upcoming lectures

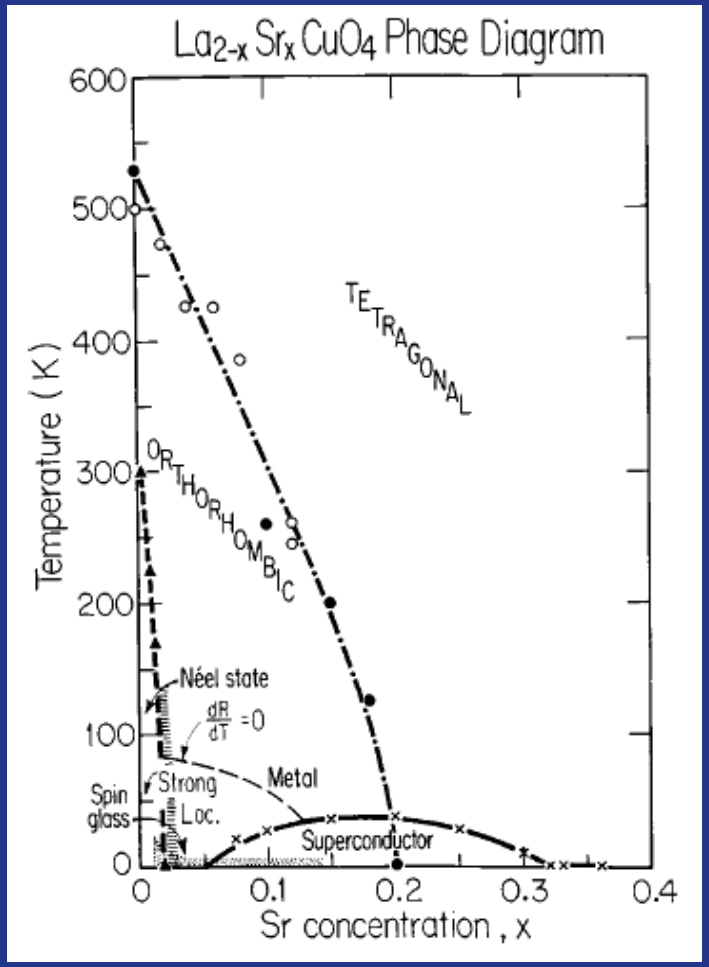

- Rapid destruction of long-range order upon hole-doping (at x ~ 2% in LSCO)

AF correlation length ~ average distance between holes ?

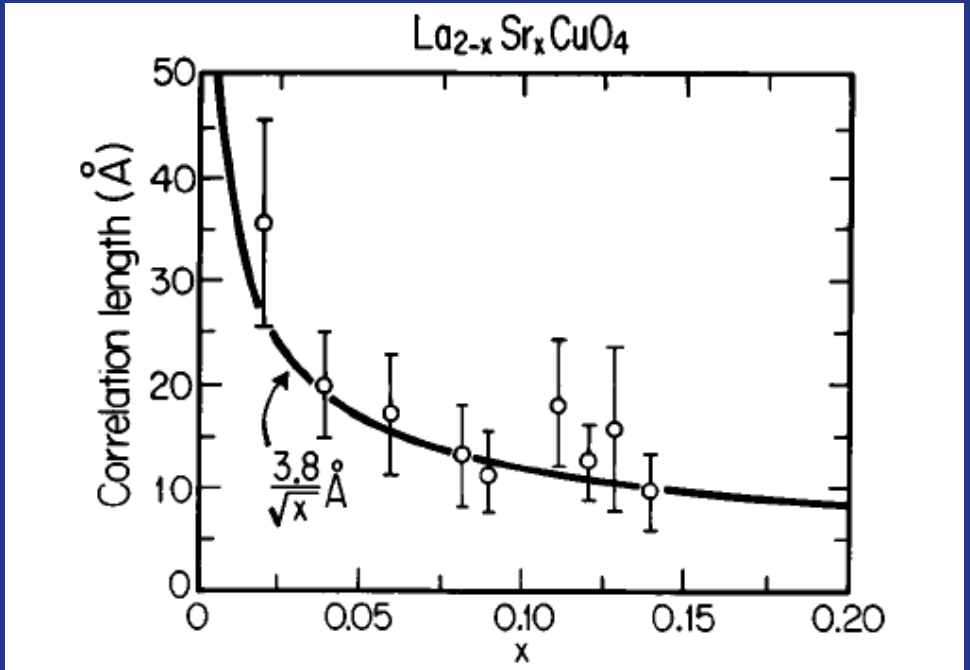

FIG. 34. Magnetic correlation length vs strontium concentration x. The curve represents the average separation between the holes introduced by doping. From Thurston, Birgeneau, Kastner *et al.* (1989).

An intriguing observation: inverse hole mobility tracks AF correlation length ? [Ando et al. PRL 87, 017001, 2001]

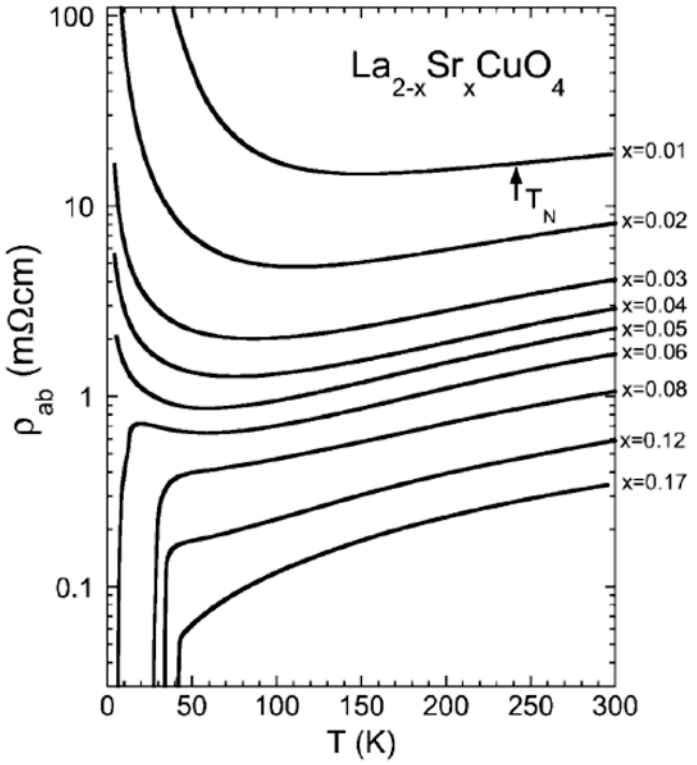

FIG. 1. Temperature dependences of ρ_{ab} in TSFZ-grown $La_{2-x}Sr_xCuO_4$ single crystals.

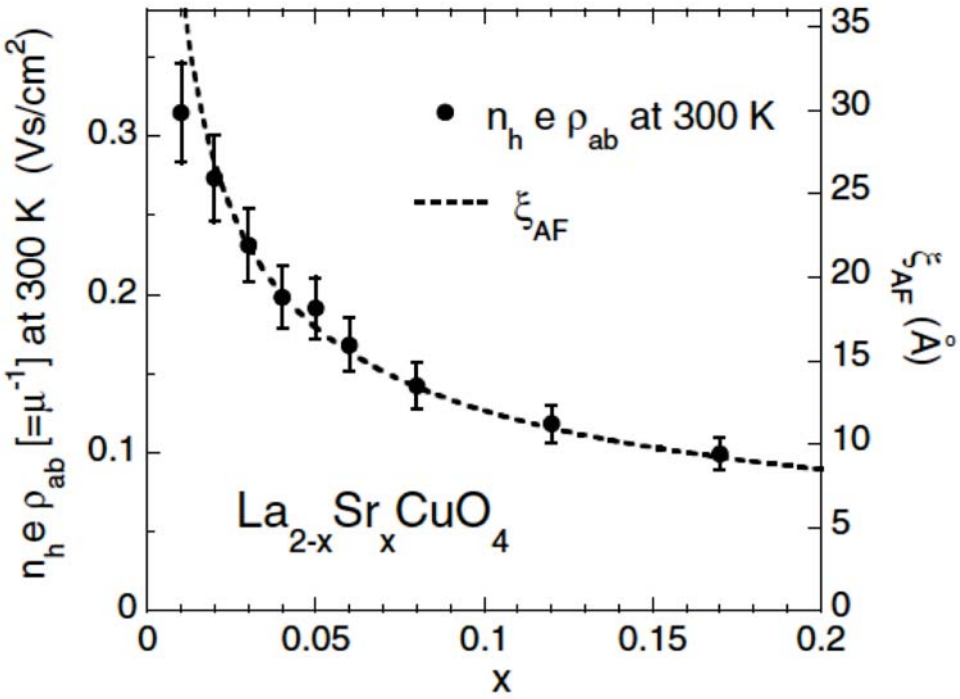

FIG. 3. x dependence of the inverse mobility (left axis) of the LSCO crystals. The dashed line shows the x dependence of ξ_{AF} (right axis), which is reported to be $3.8/\sqrt{x}$ Å by neutron experiments [5].

3. A broad overview of the different regimes

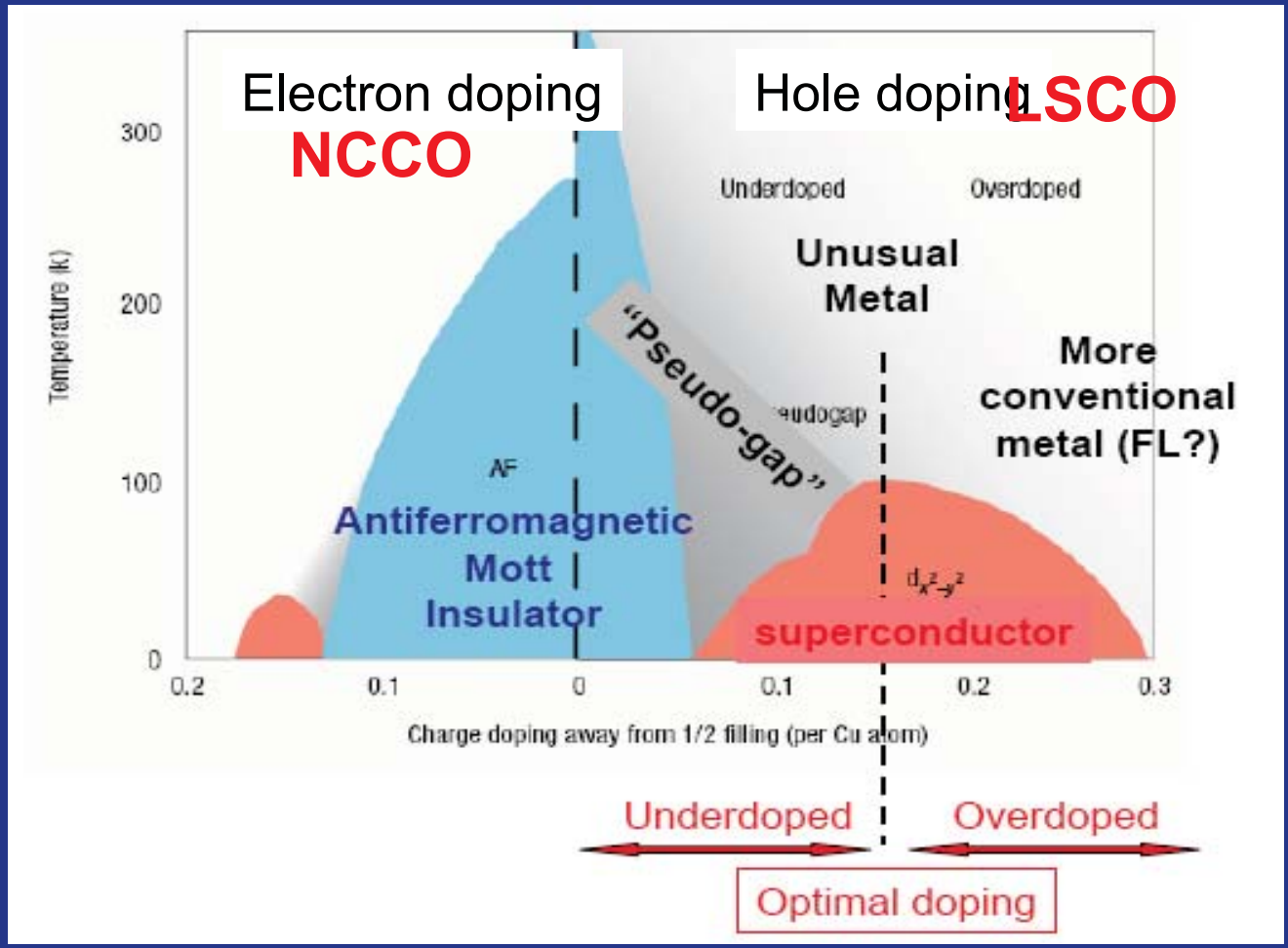

Optical conductivity

YBCO Cooper et al
PRB 47, 8233 (1993)

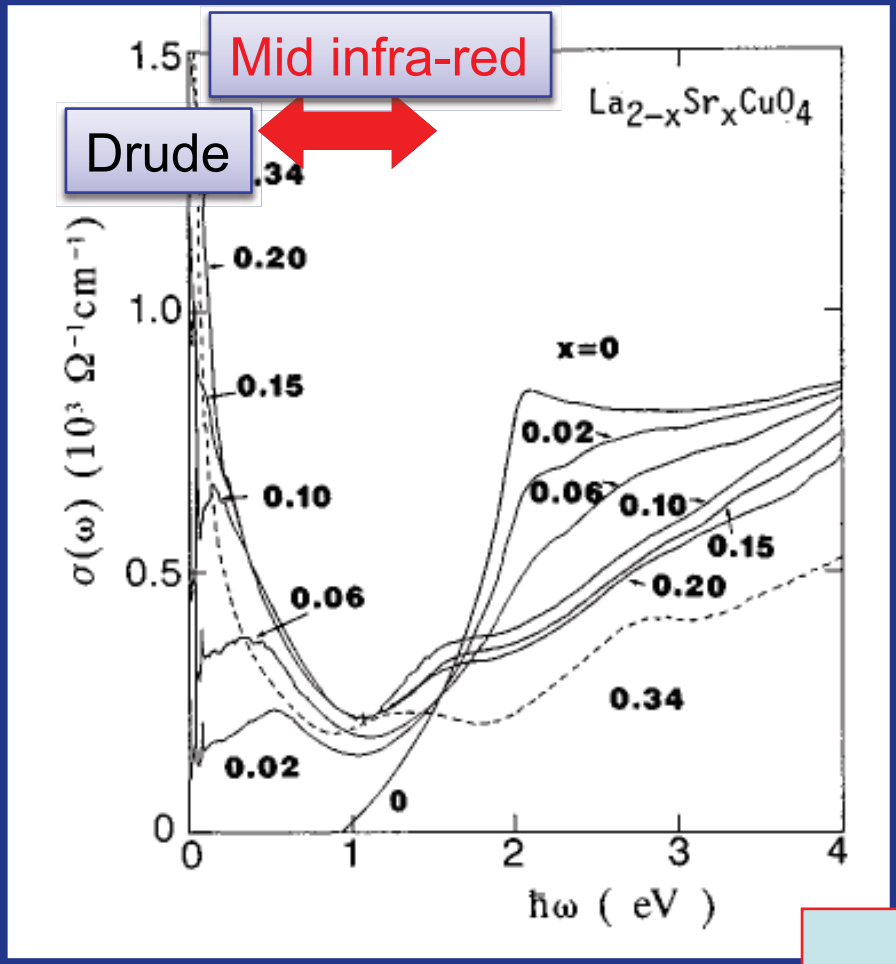

LSCO Uchida et al
PRB 43, 7942 (1991)

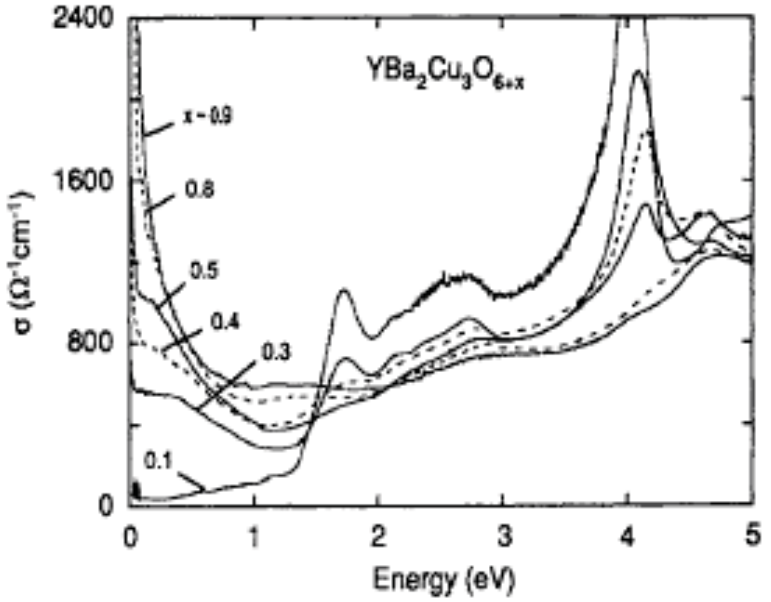

FIG. 10. In-plane ($E \perp c$) optical conductivity $\sigma(\omega)$ obtained from a Kramers-Kronig analysis of the reflectivity data for various compositions of $YBa_2Cu_3O_{6+x}$. Adapted from Cooper, Reznik, *et al.*, 1993.

- Gradual emergence of a Drude-like peak upon doping
- Large transfer of spectral weights (as x or T are varied)
- `mid infra-red' contribution

How `unconventional' is this ?
What is the number of carriers ?
(underdoped: N_{Drude} ~ x)

Optical spectral weight vs. doping

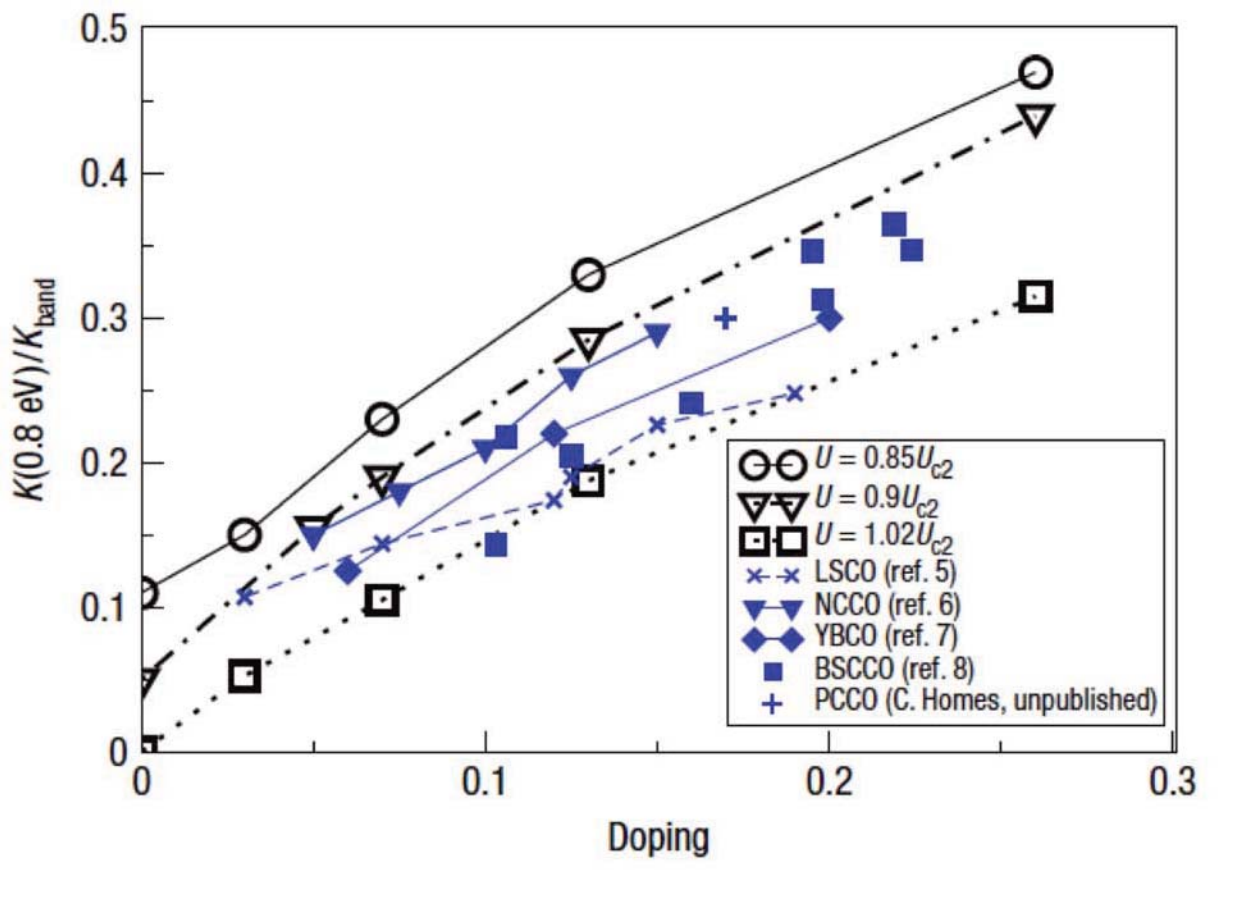

Comanac et al.
Nature Physics, 2008

Figure 3 Comparison of measured and calculated optical spectral weight. Filled symbols: spectral weight obtained by integrating experimental conductivity up to 0.8 eV from references given. Open symbols: theoretically calculated spectral weight, integrated up to $W/4$. For $U = 0.85U_{c2}$ and $U = 0.9U_{c2}$, the band-theory estimate $W = 3$ eV is used to convert the calculation to physical units; for $U = 1.02U_{c2}$, the value $W = 2.25$ eV which reproduces the insulating gap is used.

Compare with more `conventional' (3D) doped (d^1) Mott insulator: $La_{1-x}Sr_xTiO_3$

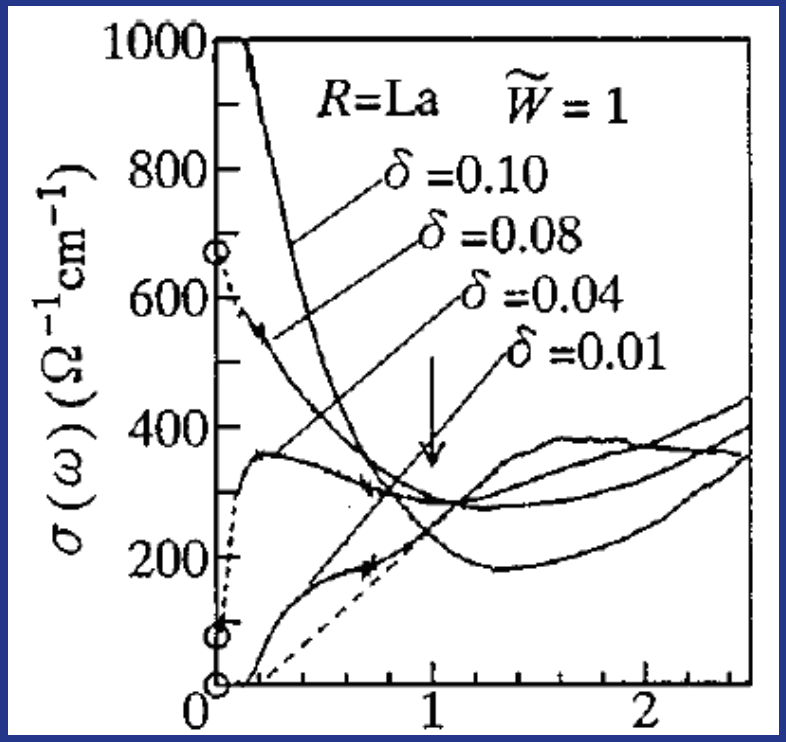

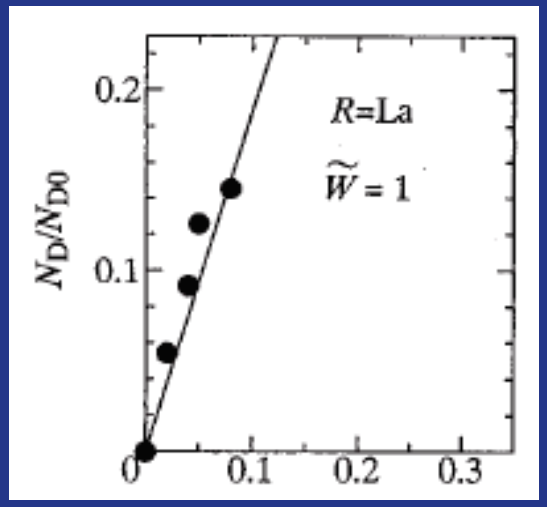

VERY SIMILAR BEHAVIOR
(at least for the main features)

You should be surprised, if you are a band-theorist (independent electrons):

- Band-theory yields a `large' Fermi surface in the paramagnetic phase for the doped system

  hole-doped w/ x holes: $\frac{A_{FS}}{A_{BZ}} = \frac{1-x}{2}$

``Luttinger volume'' (counting electron, ie filled states)

- Which NAIVELY would yield 1-x electron charge carriers (1+x hole carriers) per copper site

Can we understand this from established theories of doped Mott insulators ?... YES !

Brinkman-Rice/Gutzwiller/Slave-bosons/DMFT,
cf 2009-2010 lectures

Low-energy quasiparticles in a hole-doped Mott insulators in a phase without broken symmetry has:

- A large Fermi surface w/ Luttinger volume (1-x)/2
- Drude weight in optical conductivity $N_D \sim x$
- SMALL quasiparticle spectral weight $Z \sim x$, uniform on FS
- This defines a quasiparticle coherence scale
- Effective mass: $\frac{m^*}{m} \sim \frac{1}{J/t + x}$

$$T_F^* \sim x E_F \sim xt$$

- Fermi-liquid resistivity at low-T:

$$\rho \sim \rho_M \left(\frac{T}{T_F^*} \right)^2 + \cdots$$

This works for Titanates !

Tokura et al.
PRL, 1993

FIG. 3. The filling (x) dependence of the T linear coefficient of low-temperature specific heat (γ, closed circles) and nearly temperature-independent spin susceptibility (χ) at 300 K (open circles). In the upper part, the Wilson ratio, χ/γ normalized by $3\mu_B^2/\pi^2 k_B^2$, is plotted vs x.

Susceptibility χ and
Specific heat coefficient
C/T = γ

Beware: here x → 1-x !

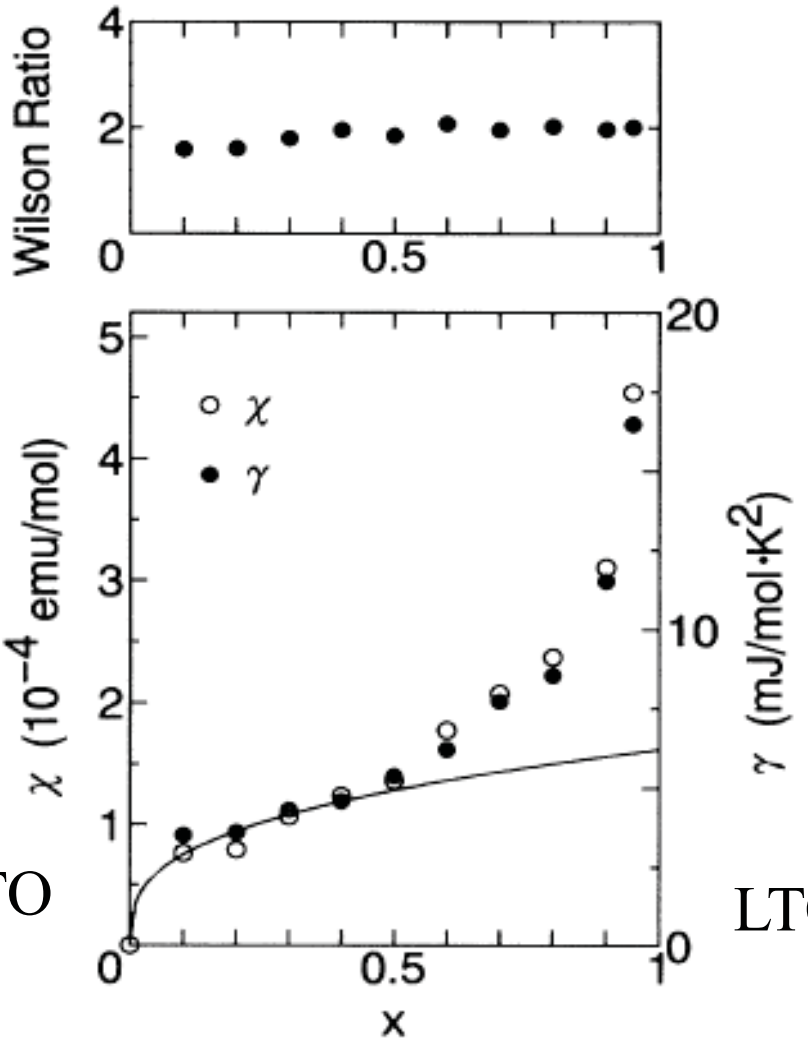

STO

LTO

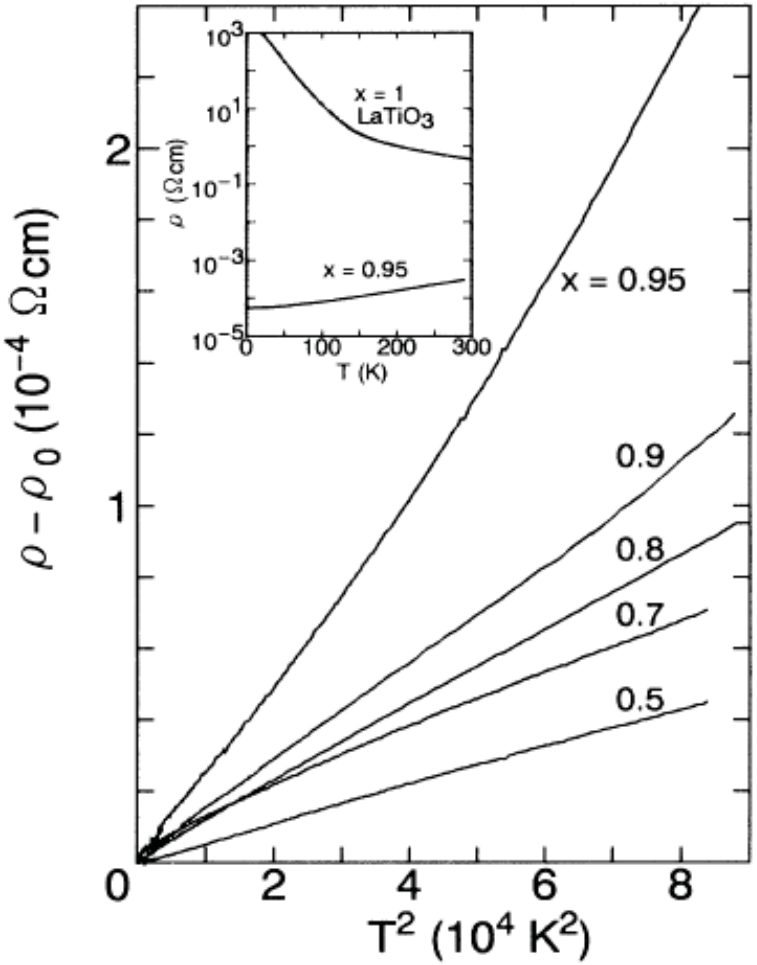

FIG. 1. Temperature (T) dependence of resistivity (ρ) in $Sr_{1-x}La_xTiO_3$. ρ is plotted vs T^2. The inset shows ρ vs T plots in the nonmetallic $x=1$ ($LaTiO_3$) and metallic $x=0.95$ samples.

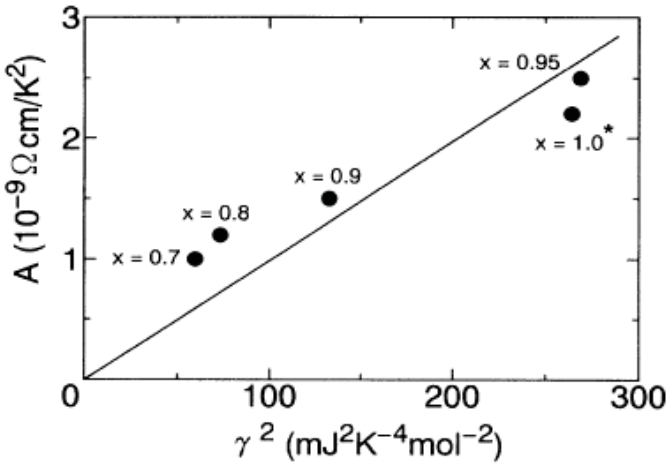

FIG. 4. The T^2 coefficient of resistivity (A) plotted vs the square of the T linear coefficient of low-temperature specific heat (γ^2) for the metallic $Sr_{1-x}La_xTiO_3$ near the metal-nonmetal phase boundary ($x \geq 0.7$). The notation $x=1^*$ indicates the nominally $x=1$ sample which is barely metallic perhaps due to a slight amount (ca. 2%) of La deficiencies.

Titanates/transport

Resistivity $\rho = AT^2 + \cdots$

Hall effect in Titanates

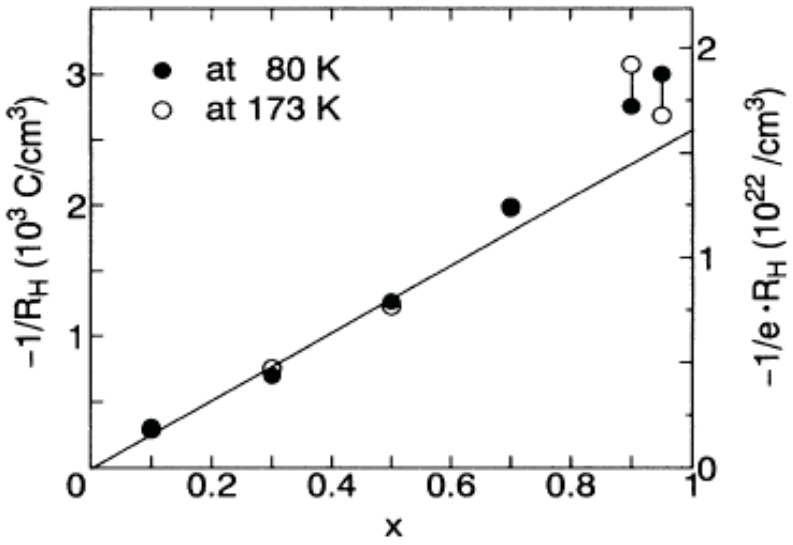

FIG. 2. The filling (x) dependence of the inverse of Hall coefficient (R_H^{-1}) in $Sr_{1-x}La_xTiO_3$. Open and closed circles represent the values measured at 80 K and 173 K, respectively. A solid line indicates the calculated one based on the assumption that each substitution of a Sr^{2+} site with La^{3+} supplies the compound with one electron-type carrier per Ti site.

Expected behavior (BR, DMFT):

Hall number is given by the total volume of the FS, NOT by the number of carriers as measured by the Drude weight

$$R_H = -\frac{1}{n_{\mathrm{FS}} e c}$$

R_H reported as almost T-independent and consistent w/ large Fermi surface

→R_H diverges in the band Insulator limit, decreases as Mott insulator is reached

Brinkman-Rice: a crash course

- theoretical intermezzo -

Consider for simplicity the infinite-U limit of the Hubbard model, i.e. the J=0 limit of the t-J model

"Slave-boson" approach: general concept:

- Enlarge Hilbert space
- Such that the constraint of no double occupancy can be enforced in an easier way (linear condition)
-And that the resulting theory is prone to mean-field approaches

(direct identification of physically relevant quasiparticles ?)

"Slave boson" b^+ such that:

$$|0\rangle \equiv b^+|\text{vac}\rangle \ , \ \ |\sigma\rangle \equiv f_\sigma^+|\text{vac}\rangle$$

subject to constraint:

$$b^+ b + \sum_\sigma f_\sigma^+ f_\sigma = 1$$

May be generalized to N spin (orbital) species $\sigma = 1, \cdots, N$:

$$b^+ b + \sum_\sigma f_\sigma^+ f_\sigma = \frac{N}{2}$$

Physical electron operator:

$$c_{i\sigma}^+ = f_{i\sigma}^+ b_i$$

Hamiltonian:

$$H = -\frac{2}{N} \sum_\sigma \sum_{ij} t_{ij} f_{i\sigma}^+ b_i b_j^+ f_{j\sigma}$$

$$S = \int_0^\beta d\tau \sum_i \left[b_i^\dagger \partial_\tau b_i + \sum_\sigma f_{i\sigma}^\dagger (\partial_\tau - \mu) f_{i\sigma} \right] - \frac{2t}{N} \int_0^\beta d\tau \sum_\sigma \sum_{ij} t_{ij} f_{i\sigma}^+ b_i b_j^+ f_{j\sigma}$$

$$+i \int_0^\beta d\tau \sum_i \lambda_i(\tau) \left[\sum_\sigma f_{i\sigma}^\dagger f_{i\sigma} + b_i^\dagger b_i - \frac{N}{2} \right] \qquad (2.20)$$

Large-N limit controlled by saddle point. b_i and λ_i fields take static, uniform expectation value (condensation of the slave-boson):

$$\langle b_i \rangle = \sqrt{\frac{N}{2}}\, r \ , \ \ i\lambda_i^* = \lambda \qquad (2.21)$$

Effective model of *free fermions* with:

$$G_f(\mathbf{k}, i\omega_n)^{-1} = i\omega_n + \mu - \lambda - r^2\, \varepsilon_{\mathbf{k}} \qquad (2.22)$$

that is:

$$\rho_f(\omega) = \frac{1}{r^2}\, D\left(\frac{\omega + \mu - \lambda}{r^2} \right) \qquad (2.23)$$

Variation w.r.t λ yields:

$$\frac{1}{N}\sum_{\sigma}\langle f_{\sigma}^{+} f_{\sigma}\rangle + \frac{r^2}{2} = \frac{1}{2} \tag{2.24}$$

If we define the doping concentration away from half-filling by: $N_f = N(1-\delta)/2$, we see that:

$$r^2 = \delta \tag{2.25}$$

Hence the slave boson condensation amplitude is directly determined by the doping.

We also note that $\mu - \lambda$ is easily found by writing that the particle number reads:

$$\langle n_{f\sigma}\rangle = \int_{-\infty}^{0} d\omega \rho_f(\omega) = \int_{-\infty}^{(\mu-\lambda)/r^2} d\varepsilon D(\varepsilon) \tag{2.26}$$

so that:

$$\boxed{\frac{\mu-\lambda}{r^2} = \mu_0(\delta)} \tag{2.27}$$

where $\mu_0(\delta)$ is the chemical potential of the *non-interacting* system, corresponding to a doping δ.

This condition insures that the Luttinger theorem is satisfied (large FS)

The physical electron Green's functions reads:

$$G_c(\mathbf{k}, i\omega_n) = \frac{Nr^2}{2} G_f(\mathbf{k}, i\omega_n) = \frac{Nr^2/2}{i\omega_n + \mu - \lambda - r^2\varepsilon_{\mathbf{k}}} \tag{2.28}$$

while the non-interacting Green's function reads (remember that the hopping was scaled by $2/N$):

$$G_c^0(\mathbf{k}, i\omega_n) = \frac{1}{i\omega_n + \mu - 2\varepsilon_{\mathbf{k}}/N} \tag{2.29}$$

so that the self-energy reads:

$$\Sigma_c \equiv \left[G_c^0\right]^{-1} - \left[G_c\right]^{-1} = \mu - \frac{2}{N}\mu_0(\delta) + i\omega_n \left(1 - \frac{2}{Nr^2}\right) \tag{2.30}$$

We see that it depends only on frequency, in a very simple manner. The constant term insures Luttinger's theorem, as discussed above: $\mu - \Sigma_c(0) = \epsilon_F^0$, with $\varepsilon_F^0 = 2\mu_0(\delta)/N$ the Fermi level of the physical electrons in the non-interacting system. The linear term yields the quasi-particle residue:

Quasiparticle weight :

$$Z = \frac{N}{2} r^2 = \delta \ \ (\text{for N} = 2)$$

Effective mass :

$$\frac{m^*}{m} = \frac{1}{Z} = \frac{1}{\delta}$$

Brinkman-Rice:

Large Fermi surface

(consistent with Luttinger theorem counting electrons)

Quasiparticle spectral weight vanishes at small doping

QP effective mass diverges (regularized by J, see next lecture)

Spectral weight transfers in optics: Dynamical Mean-Field Theory calculations

(need to go beyond simple BR)

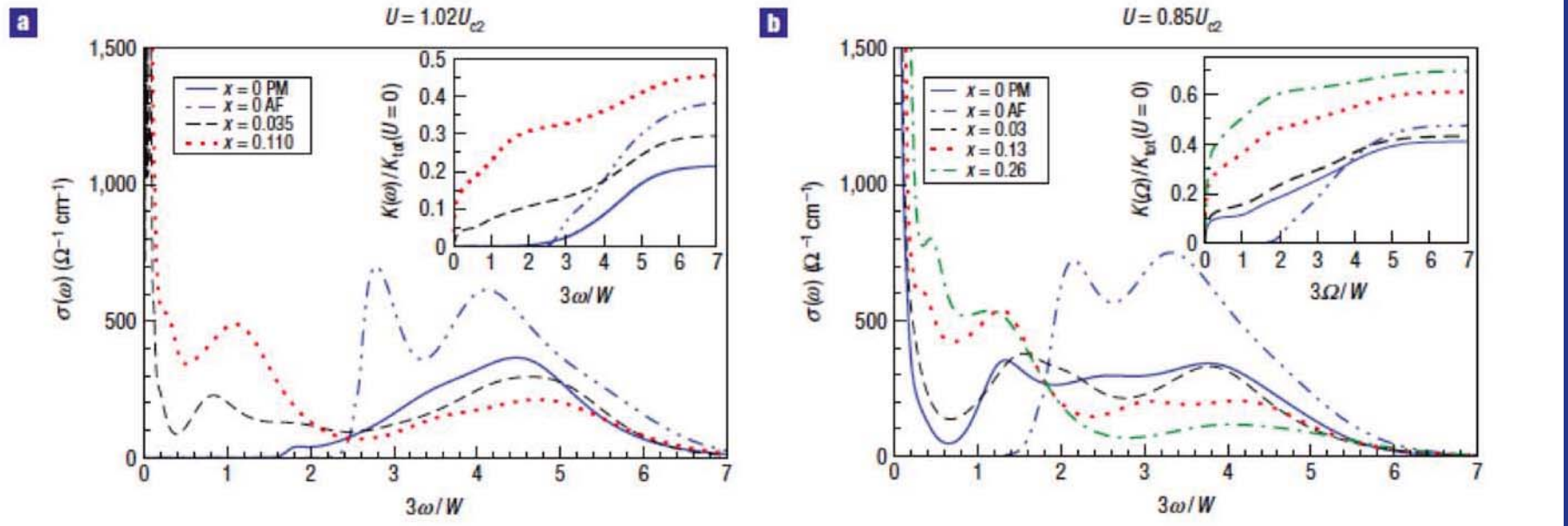

Figure 1 Optical conductivity of Hubbard model. Calculated as described in the main text at dopings $x = 1 - n$ and interaction strength U indicated. **a**,**b**, Optical conductivity. Insets: Optical integral. For $x = 0$, both paramagnetic (PM) and antiferromagnetic (AF) phase calculations are shown; for $x > 0$, only paramagnetic phase results are given. If the band theory value $W = 3$ eV is used then the frequency scale is electronvolts.

Comanac et al.

Although some aspects of cuprates
(Drude weight, main features and transfers of spectral weight in optics)
fit with established theories
of doped Mott Insulators (BR, local DMFT),
several key aspects of cuprates
STRONGLY DEPART FROM IT…

→ ***Cuprates take a rather unique route for the emergence of a metal out of a Mott insulator***

Hall effect: strongly non Brinkman-Rice!

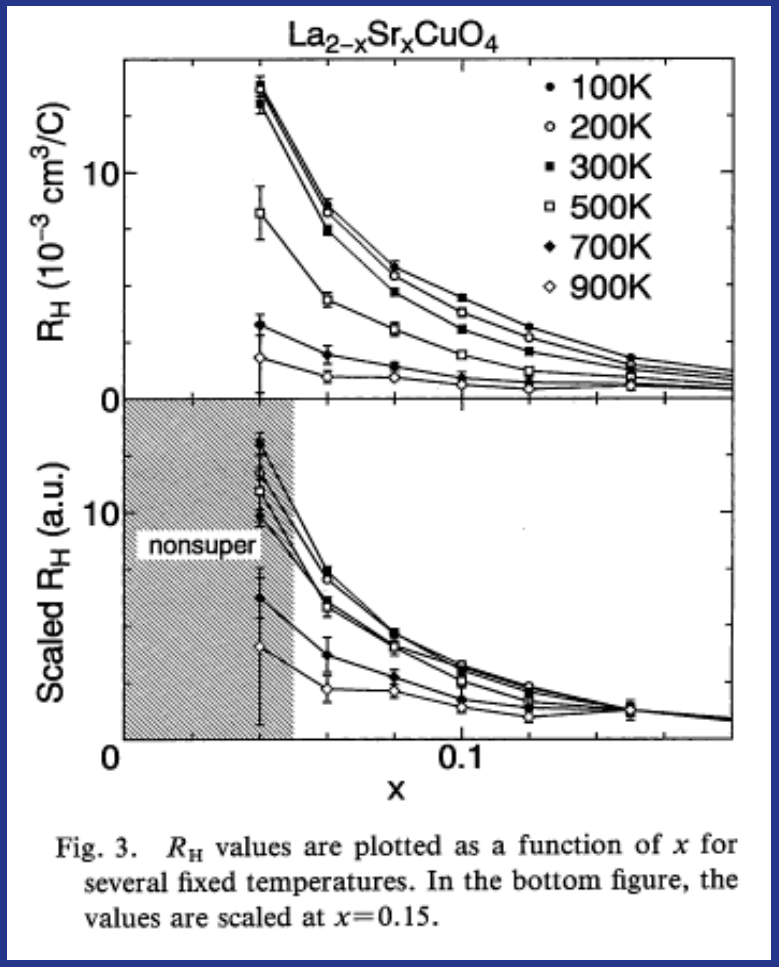

Fig. 3. R_H values are plotted as a function of x for several fixed temperatures. In the bottom figure, the values are scaled at $x=0.15$.

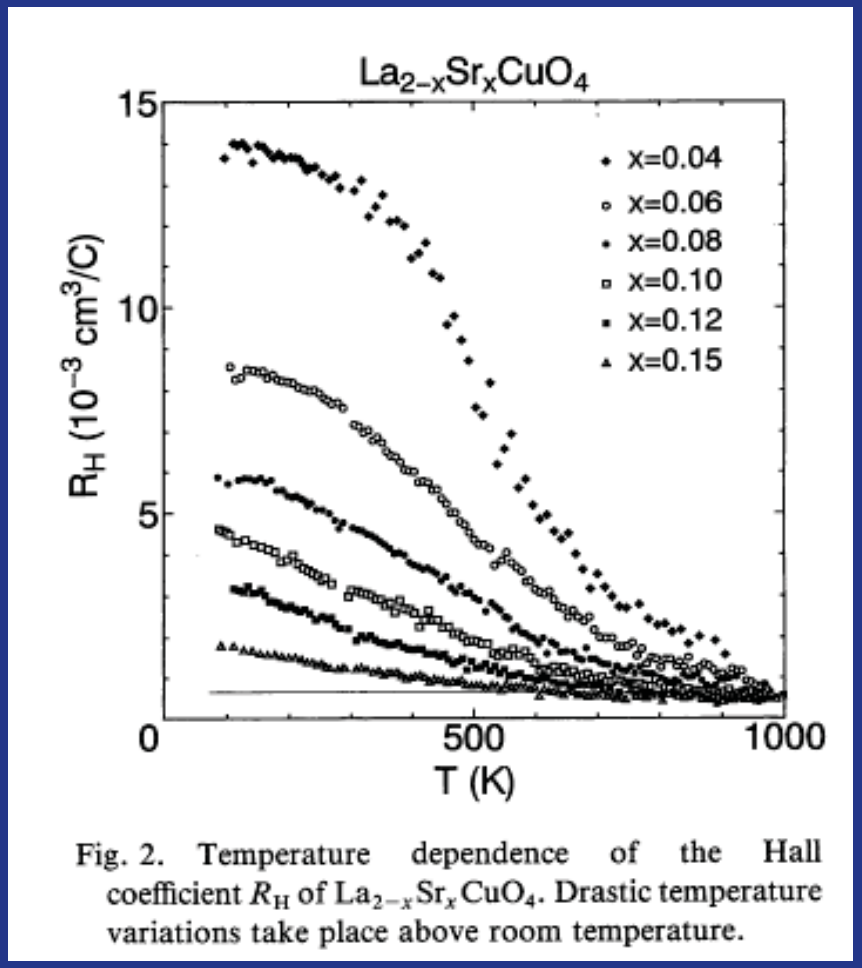

Fig. 2. Temperature dependence of the Hall coefficient R_H of $La_{2-x}Sr_xCuO_4$. Drastic temperature variations take place above room temperature.

Nishikawa et al. 1994
Hwang et al, 1994

R_H becomes LARGE as doping is reduced at low-T

Inconsistent w/ large Fermi surface picture

Strongly T-dependent when considered over wide range

Hall number scaled by number of HOLES

A beautiful study

(Ando et al. PRL 92, 197001 (2004))

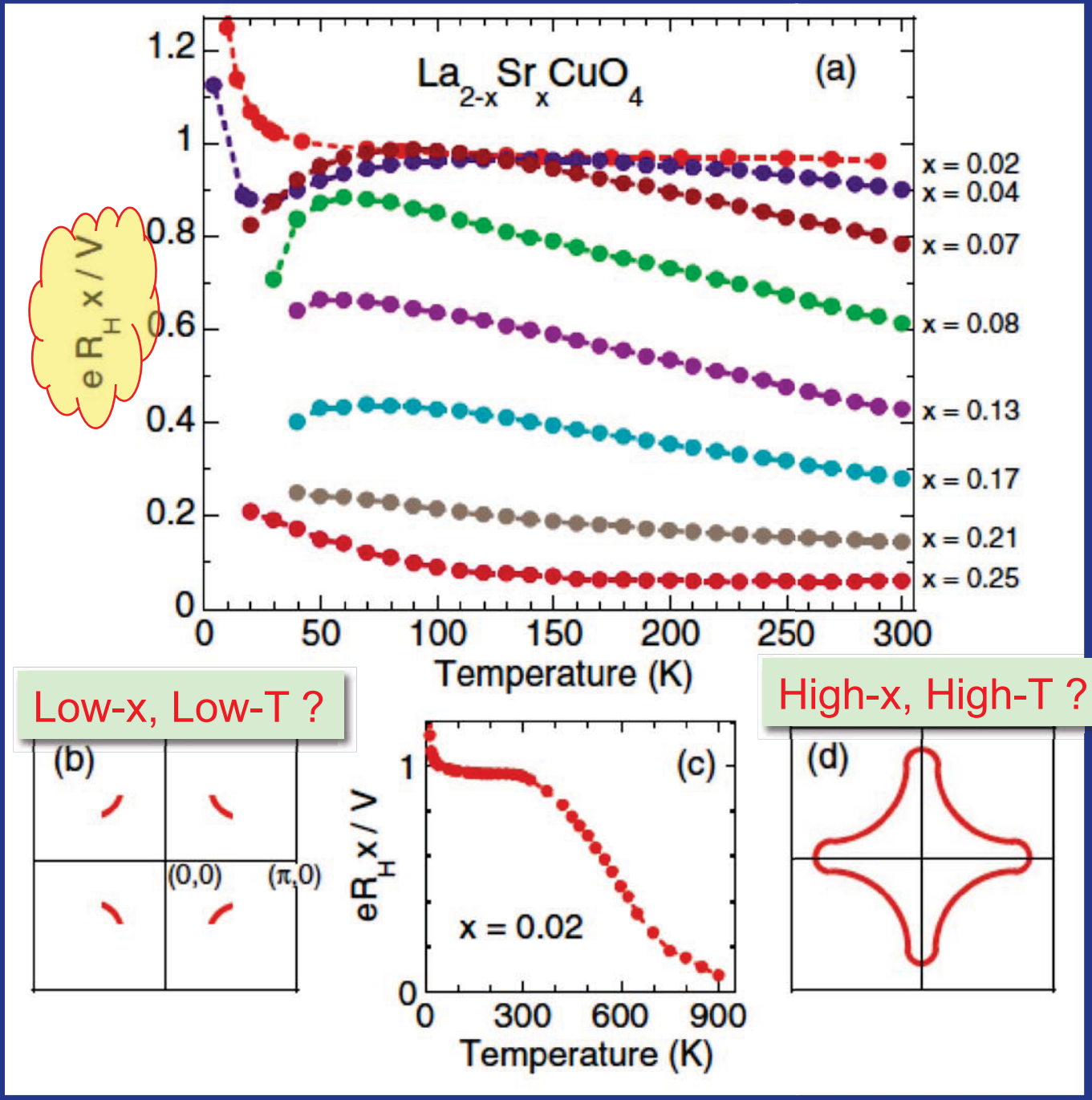

The « pseudogap »:

partial truncation of the Fermi surface at low doping level

Bad things seem to happen to quasiparticles in the underdoped normal state !

Cuprate
= quasiparticlebuster

Quasiparticle

*See*ing quasiparticles: Angle-Resolved Photoemission Spectroscopy (ARPES) :

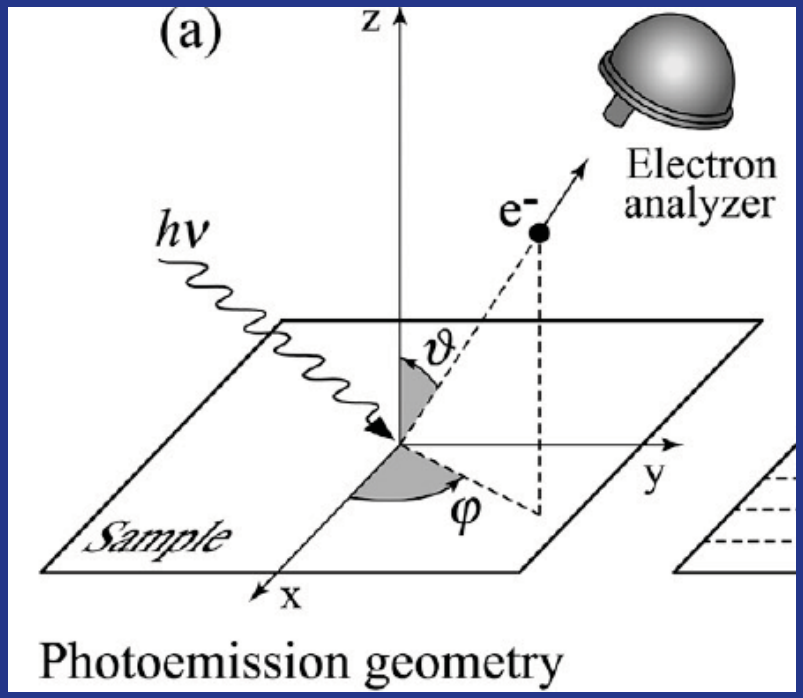

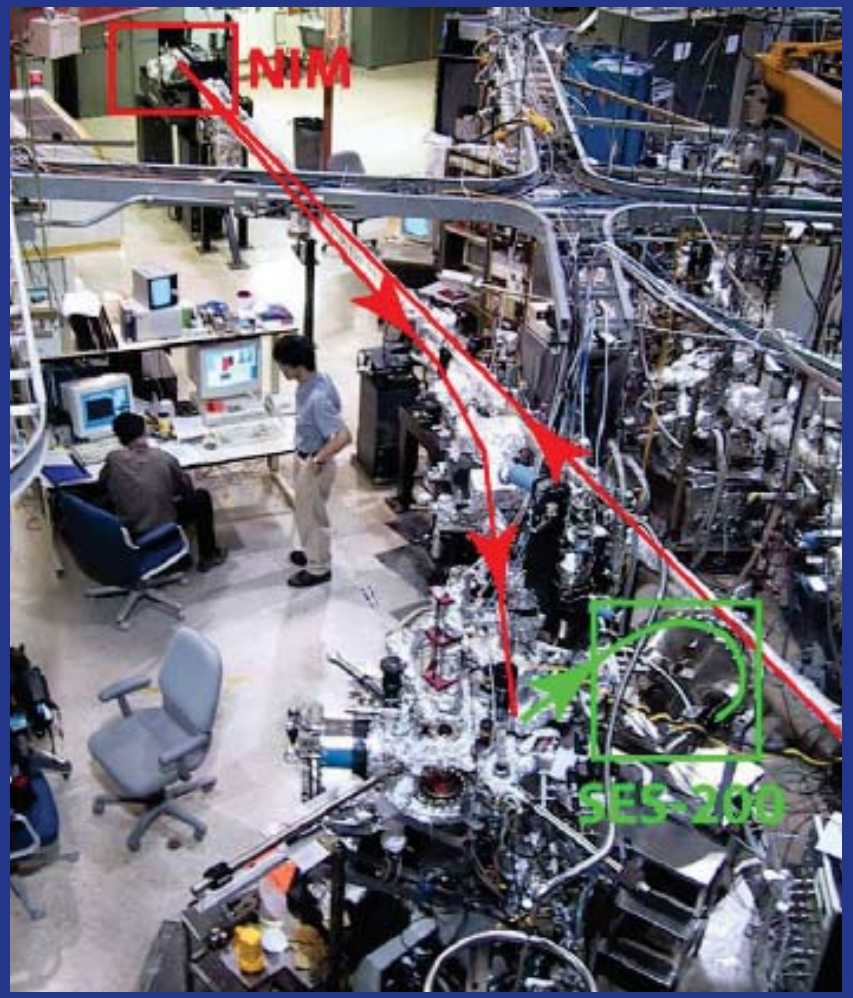

Buckley prize 2011

To: Campuzano, Johnson, Shen

The one-particle spectral function: injecting/removing an extra particle in a many-body system

$$A(\mathbf{k},\omega) = \sum_n |\langle \Psi_n^{N-1}|\psi_{\mathbf{k}}|\Psi_0^N\rangle|^2\,\delta(\omega+\mu+E_n-E_0)$$

$$A = A_{\mathrm{QP}} + A_{\mathrm{inc}}$$

= Slow + Fast

$$A_{\mathrm{QP}}(\mathbf{k},\omega) \simeq Z_{\mathbf{k}} \frac{\Gamma_{\mathbf{k}}}{\pi[(\omega-\xi_{\mathbf{k}})^2+\Gamma_{\mathbf{k}}^2]}$$

QP peak

Incoherent

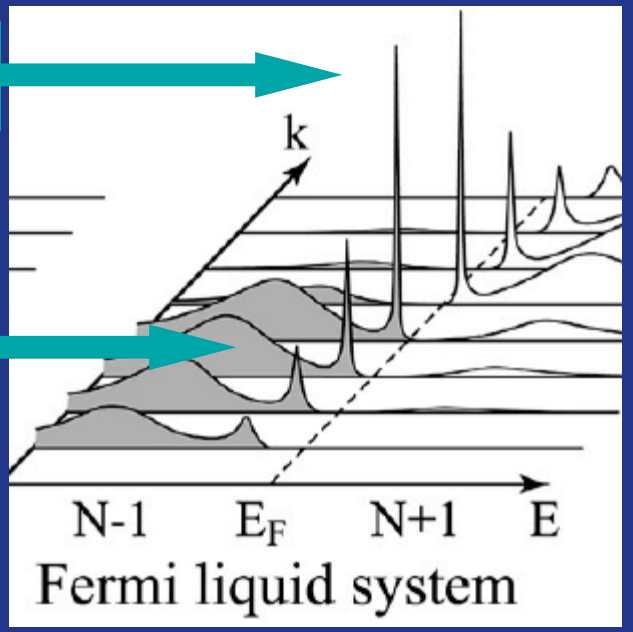

NORMAL state:

- ``Nodal'' regions display reasonably coherent quasiparticles
- In contrast, excitations in the ``antinodal'' regions e.g. (0,π) are much more incoherent

  AND they are (pseudo-) gapped below T*

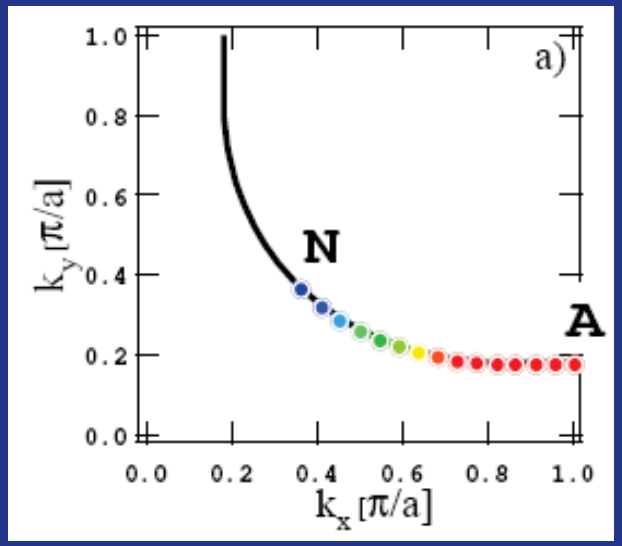

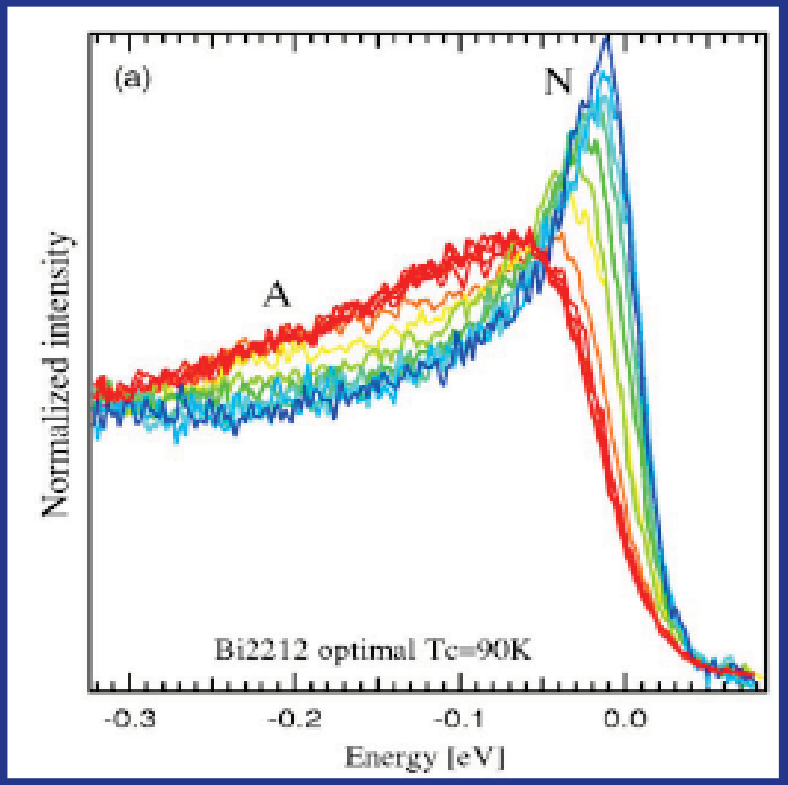

Kaminski et al.,
PRB 71, 014517 (2005)

Bi2212 Tc=90K@T=140K

ARPES sees « Fermi arcs »

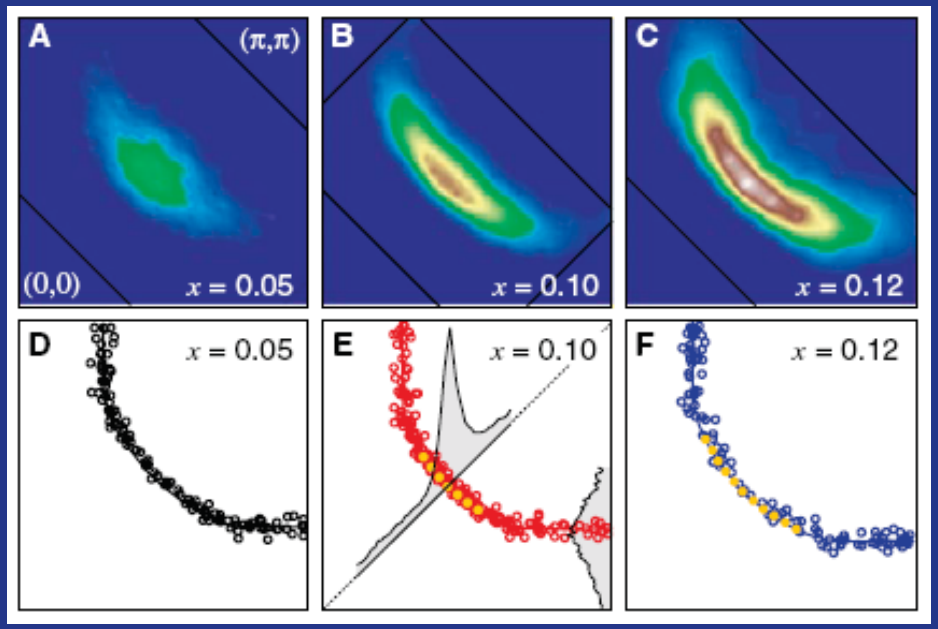

$Ca_{2-x}Na_xCuO_2Cl_2$

K.Shen et al. Science 2007

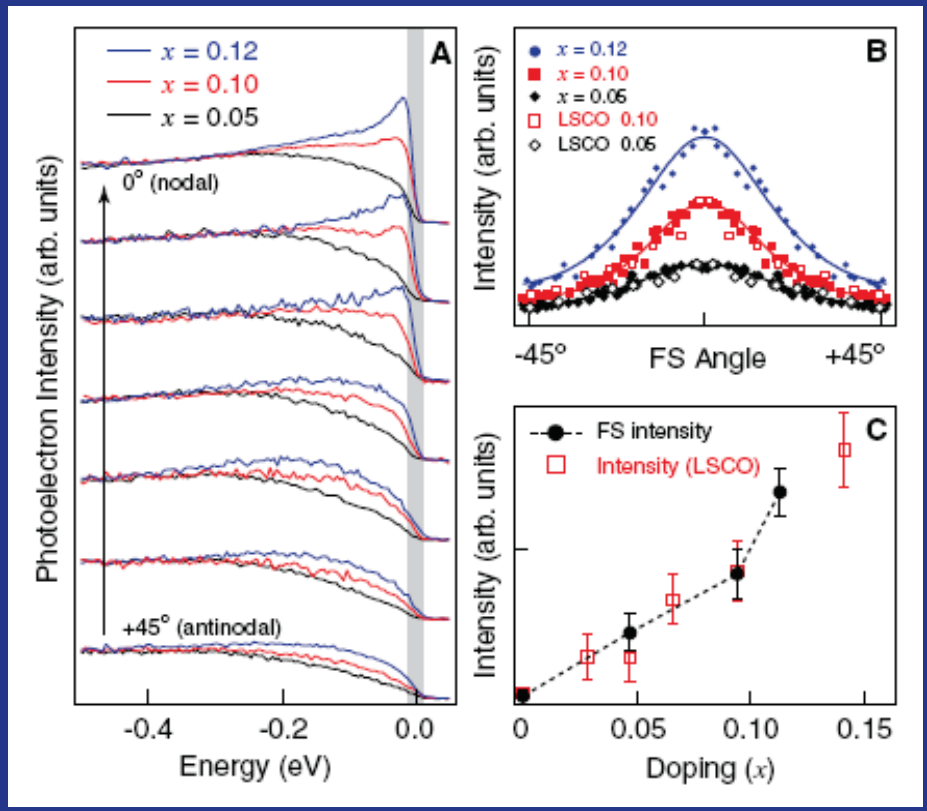

SUPERCONDUCTING state:

* Antinodal quasiparticles make a comeback

(Note: still they remain somewhat fragile and have very small spectra weight at very low doping… cf also Vishik et al., Nature Physics 2009)

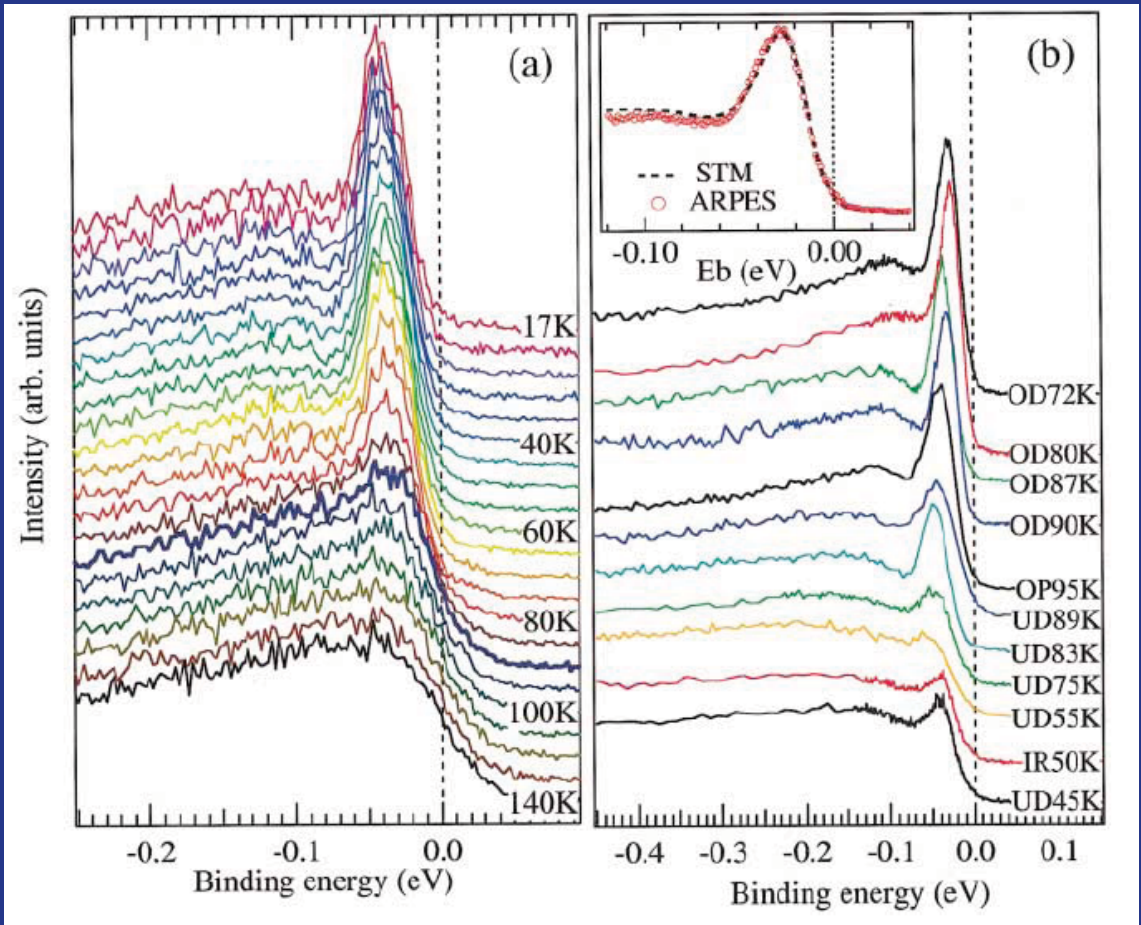

FIG. 1 (color). (a) ARPES spectra at $(\pi, 0)$ of slightly overdoped Bi2212 ($T_c = 90$ K) for different temperatures ($T = 17$, 20, 25, 30, 35, 40, 45, 50, 55, 60, 65, 70, 75, 80, 85, 90, 95, 100, 110, 120, 130, and 140 K). (b) Spectra at $(\pi, 0)$ at low T (14 K) of differently doped Bi2212 samples (OD—overdoped; OP—optimally doped; UD—underdoped; IR—300 MeV electron irradiated, followed by the value of T_c). Intensity of the spectra is normalized at a high binding energy where the spectral intensity shows a minimum (~ -0.5 eV). Inset: Comparison between low-T ARPES at $(\pi, 0)$ and STM for the same OD72K sample.

Ding et al. PRL 2001

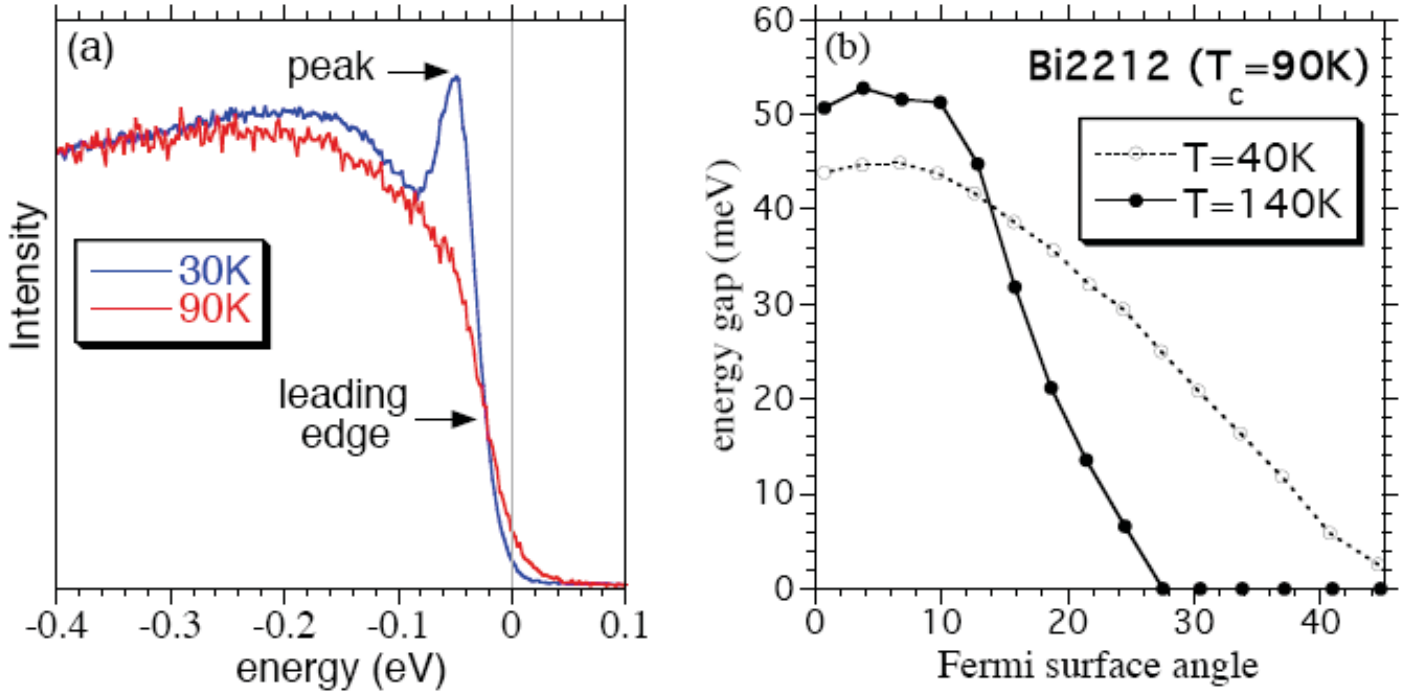

Figure 5 – (a) ARPES spectrum at (π,0) for an underdoped Bi2212 sample in the superconducting state (30K) and the pseudogap phase (90K). The sharp peak in the superconducting state is replaced by a leading edge gap in the pseudogap phase. (b) Angular anisotropy of the superconducting gap (40K) and the pseudogap (140K) for an optimal doped Bi2212 sample. Data courtesy of Adam Kaminski and Juan Carlos Campuzano.

Take-home message/ARPES:

- Strong Nodal/Antinodal dichotomy in the normal state
- Possibly extends also for Bogoliubov QPs in the SC state
- Gradually (?) becomes more uniform in momentum space as we enter the overdoped regime

Phenomenology of the pseudogap state (cont'd) :

- Magnetic response (NMR)

- Specific heat

- Signatures in other spectroscopies:
(c-axis optics and transport, STM, …

For reviews, see:
-Timusk and Statt, Rep.Prog.Phys 1999
- Norman et al. Adv Phys 2005

Discovery of the PG – NMR -1989
Depletion of magnetic excitations at T*

See in particular: Alloul, Ohno and Mendels, PRL 63, 1700 (1989)

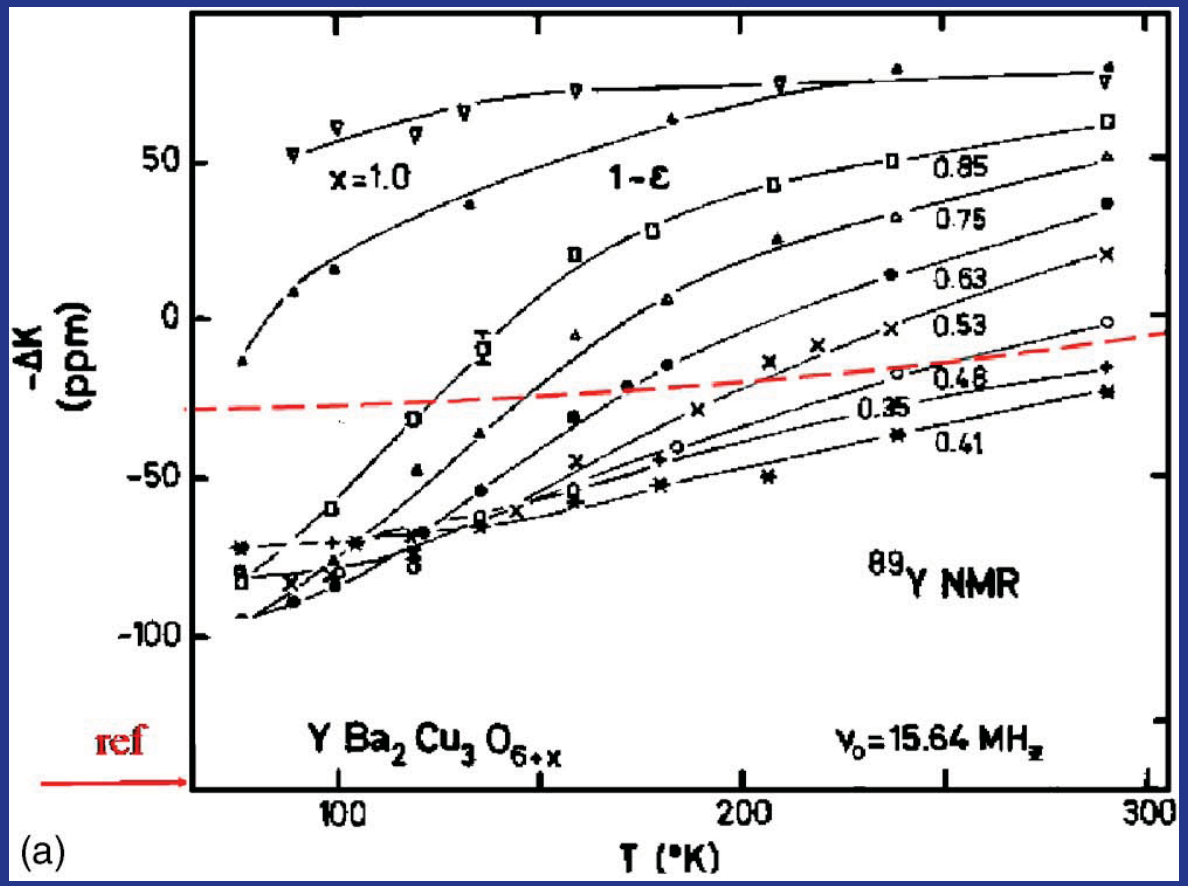

----------:
Heisenberg model

Baseline
(orbital contrib.
Substracted)

Doping-dependence of PG scale T*

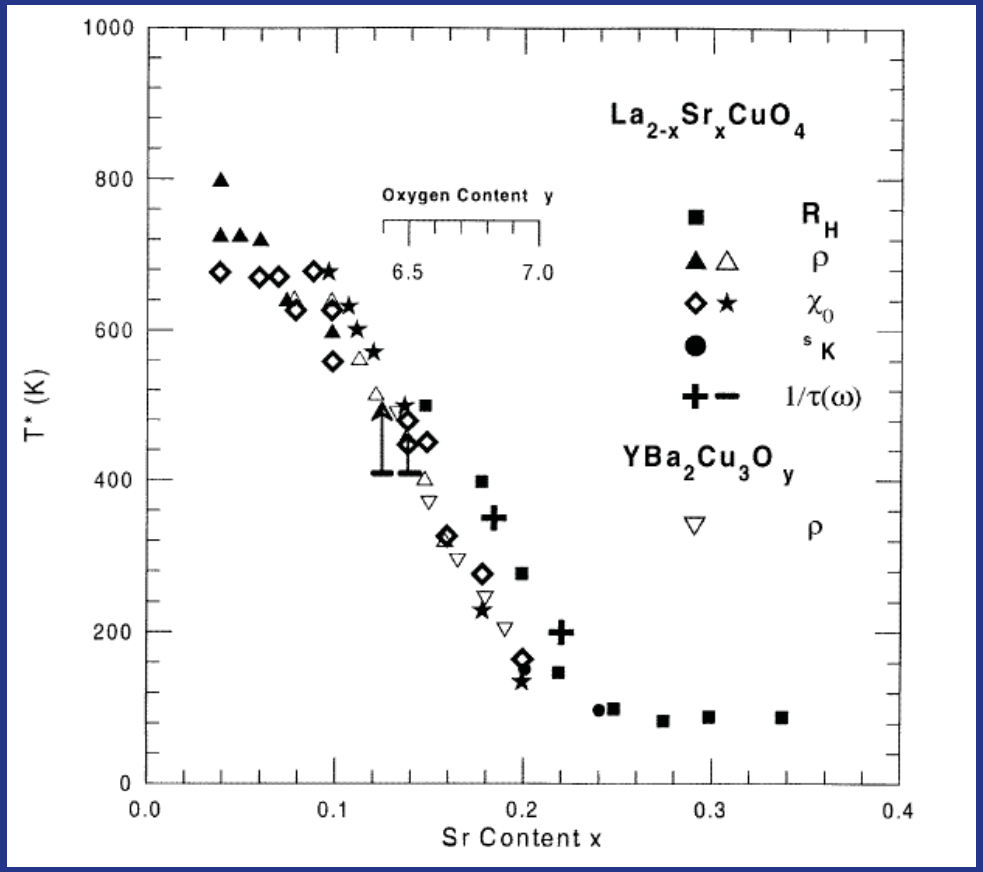

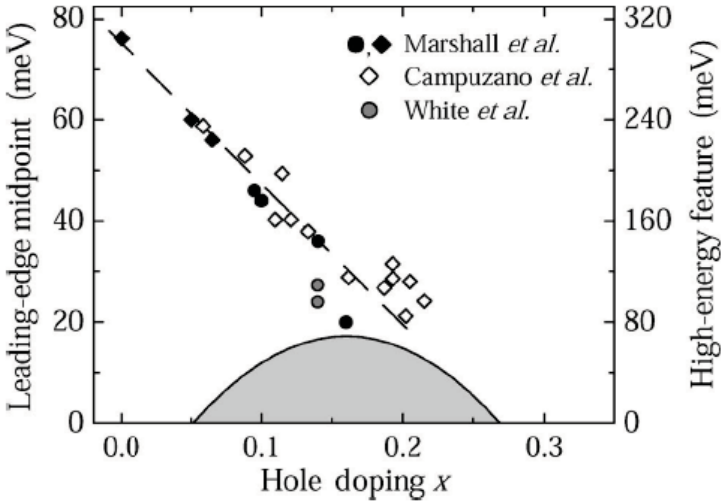

FIG. 62. Doping dependence of the pseudogap as determined by the position of leading-edge midpoint (circles, left axis) and high-energy feature (diamonds, right axis) in the $(\pi,0)$ ARPES spectra from $Bi_2Sr_2CaCu_2O_{8+\delta}$ (Bi2212) [the dome represents the d-wave mean-field approximation $\Delta(x)=4.3k_BT_c(x)/2$, left scale (Won and Maki, 1994)]. Data from Marshall *et al.* (1996); White *et al.* (1996); Campuzano *et al.*, (1999).

Figure 26. Variation of T^* with doping for $La_{2-x}Sr_xCuO_4$ as measured by various probes. The full squares denote the temperature below which the Hall coefficient has a rapid temperature dependence. The open circles refer to maxima in the static susceptibility $\chi(T)$ and the full circles the temperature where the Knight shift starts to decrease. The triangles refer to the temperature where there is a slope change in the dc resistivity, the crosses infrared measurements of $1/\tau$ supression and the horizonatal lines to lower limits of infrared data.

Specific heat

(Loram, Cooper et al.) cf. also L.Perfetti et al. `pump-probe calorimetry', 2009

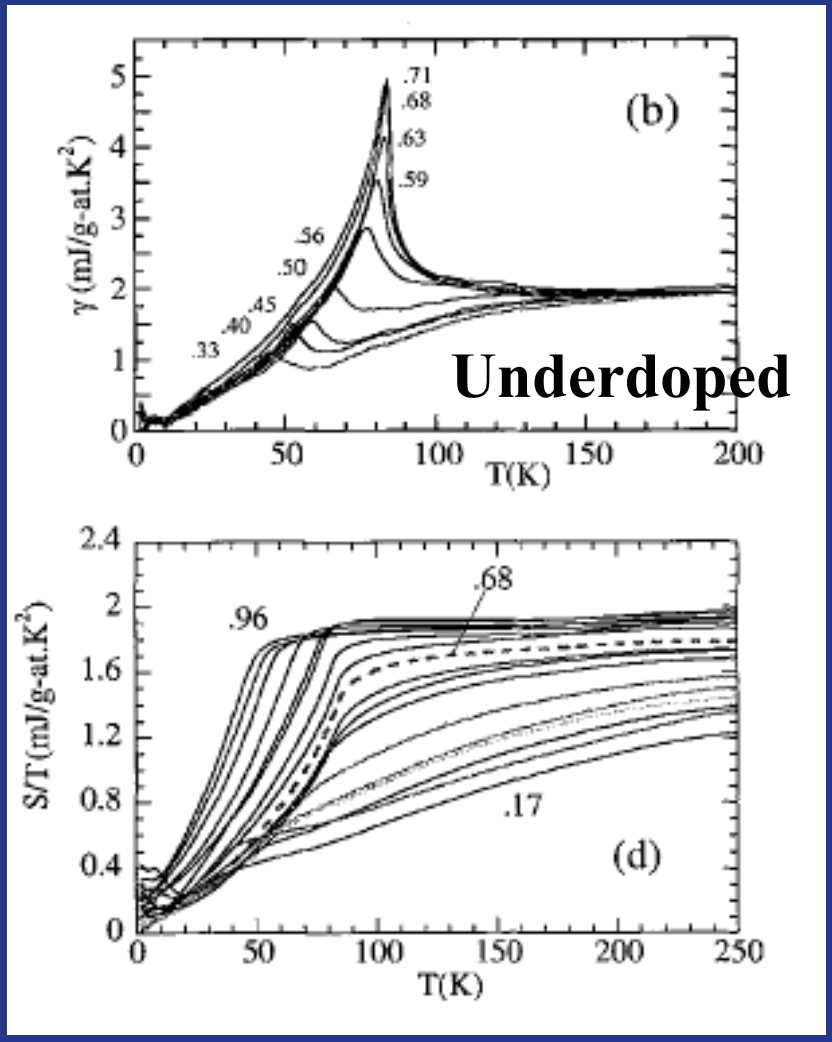

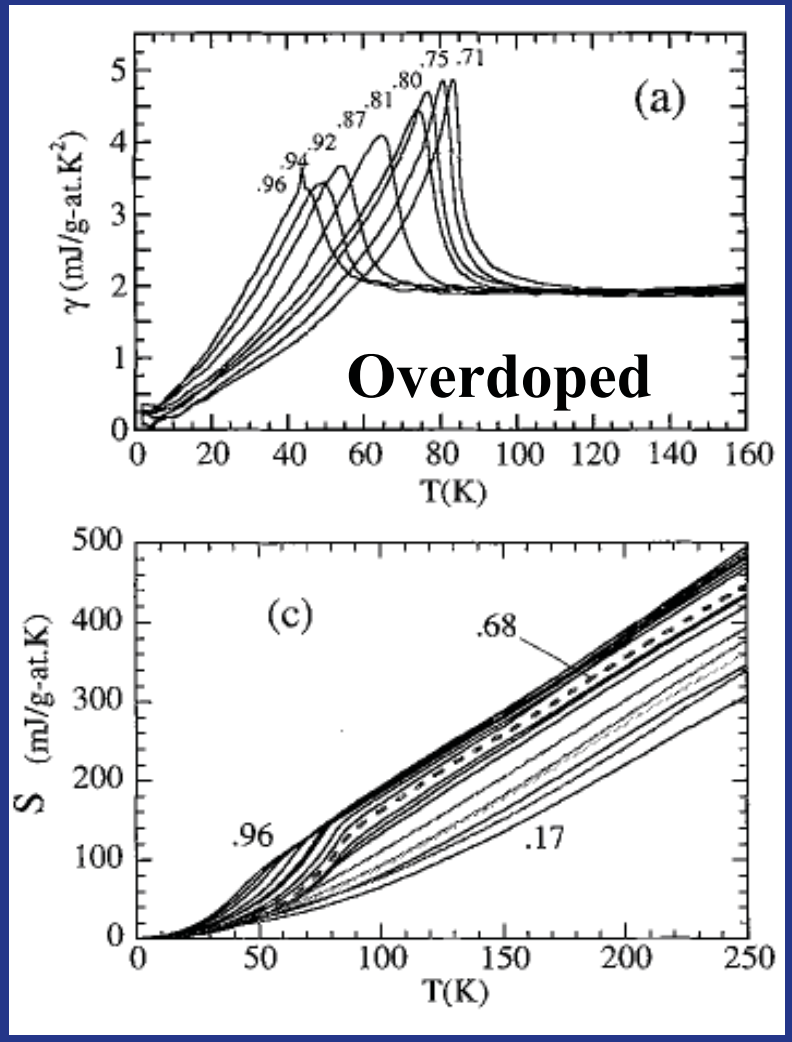

$\gamma(T)=C/T$ coefficient:

- Is not severely enhanced close to insulator

(OK w/ the notion that J/t sets the effective mass and cuts off the divergence w/doping)

- BUT shows depletion at a temperature $T^*>T_c$ for underdoped compounds

(i.e γ becomes T-dependent)

c-axis optics and transport

Basov et al.

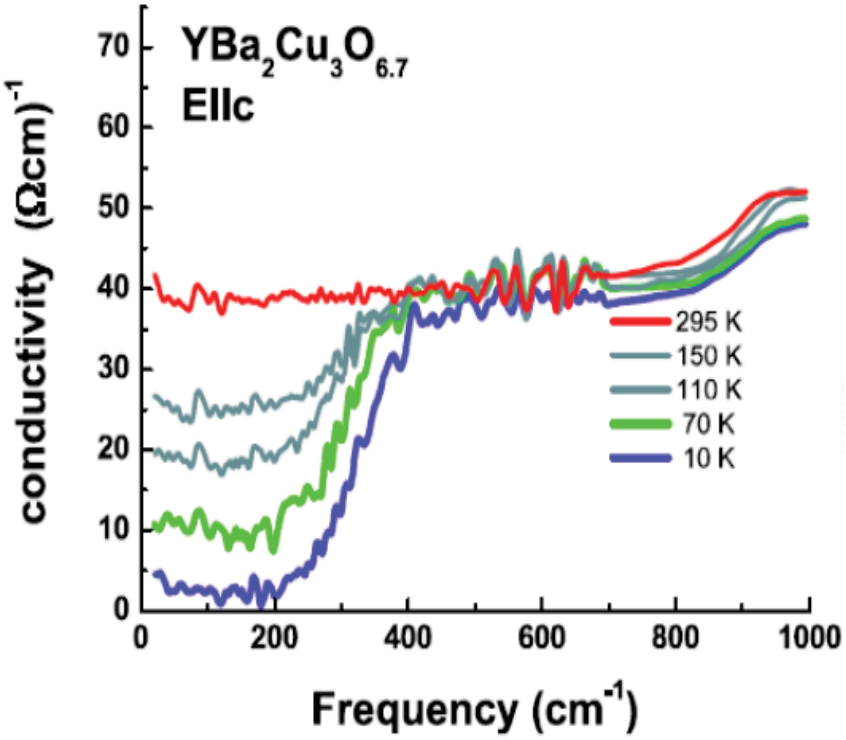

Figure 4 – c-axis conductivity (phonon subtracted) for underdoped YBCO, with a pseudogap that fills in with increasing temperature [21]. Figure courtesy of Dmitri Basov.

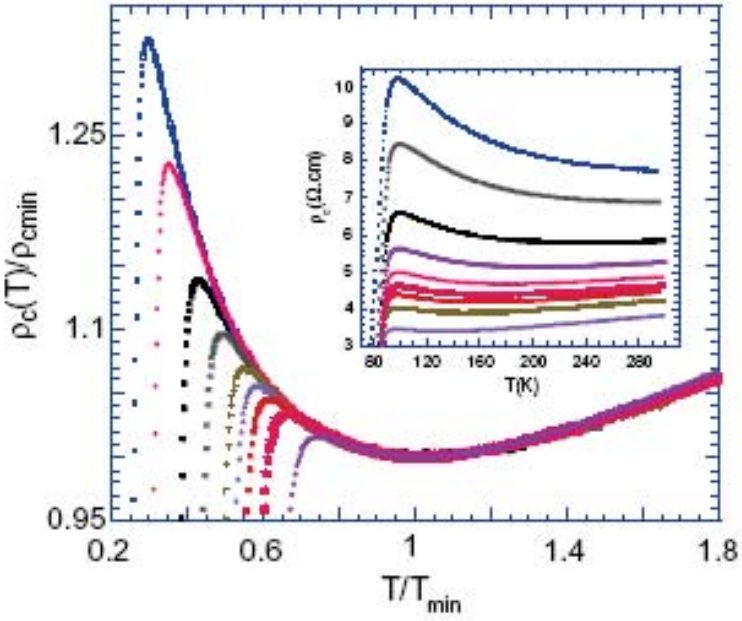

Fig. 3. Scaling of $\rho_c(T)$, shown in the insert, measured at various doping, normalized by its value ρ_{cmin} at T_{min}, vs T/T_{min}.

Raffy et al.

Single-particle spectroscopies: PG from STM tunneling spectra

Main features:

- **A dip at low voltage (pseudogap)**
- **Opens well above T_c in ubderdoped samples**
- **An overall particle-hole asymmetry**

Renner et al., PRL (1998)
See review by Fischer et al Rev Mod Phys 2007

→ See seminar by C.Berthod

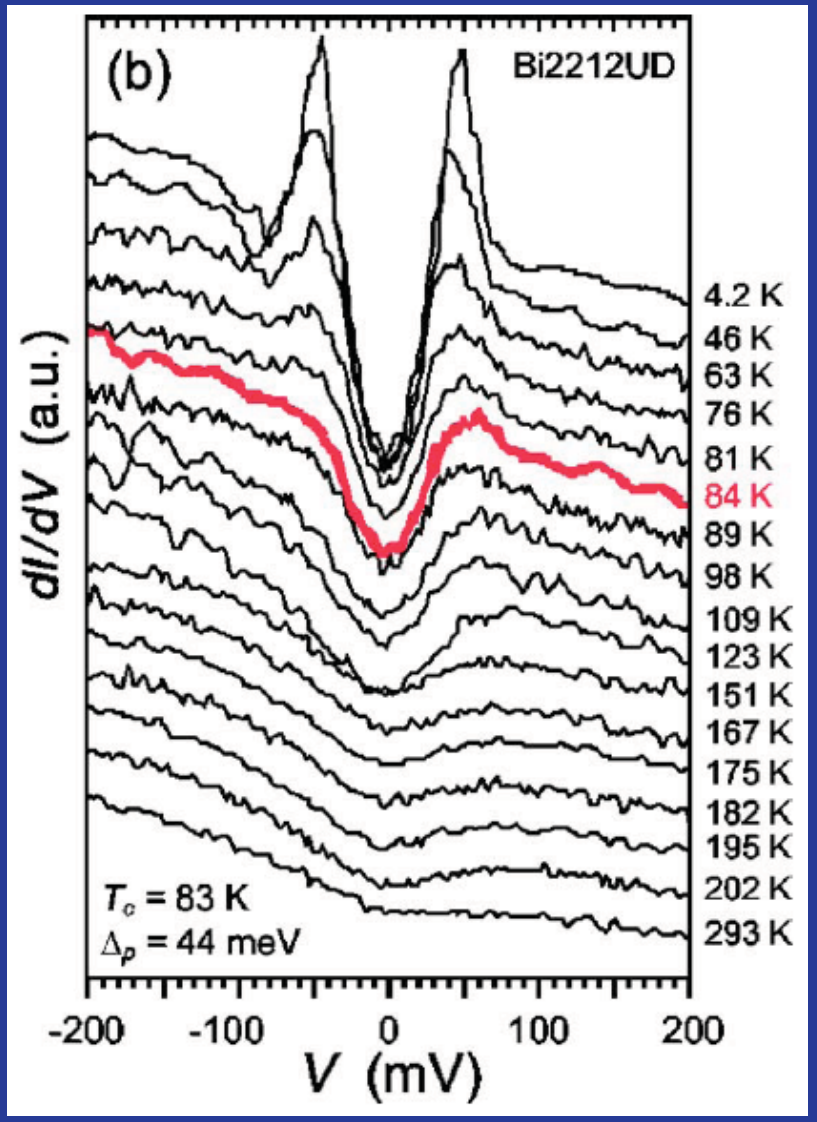

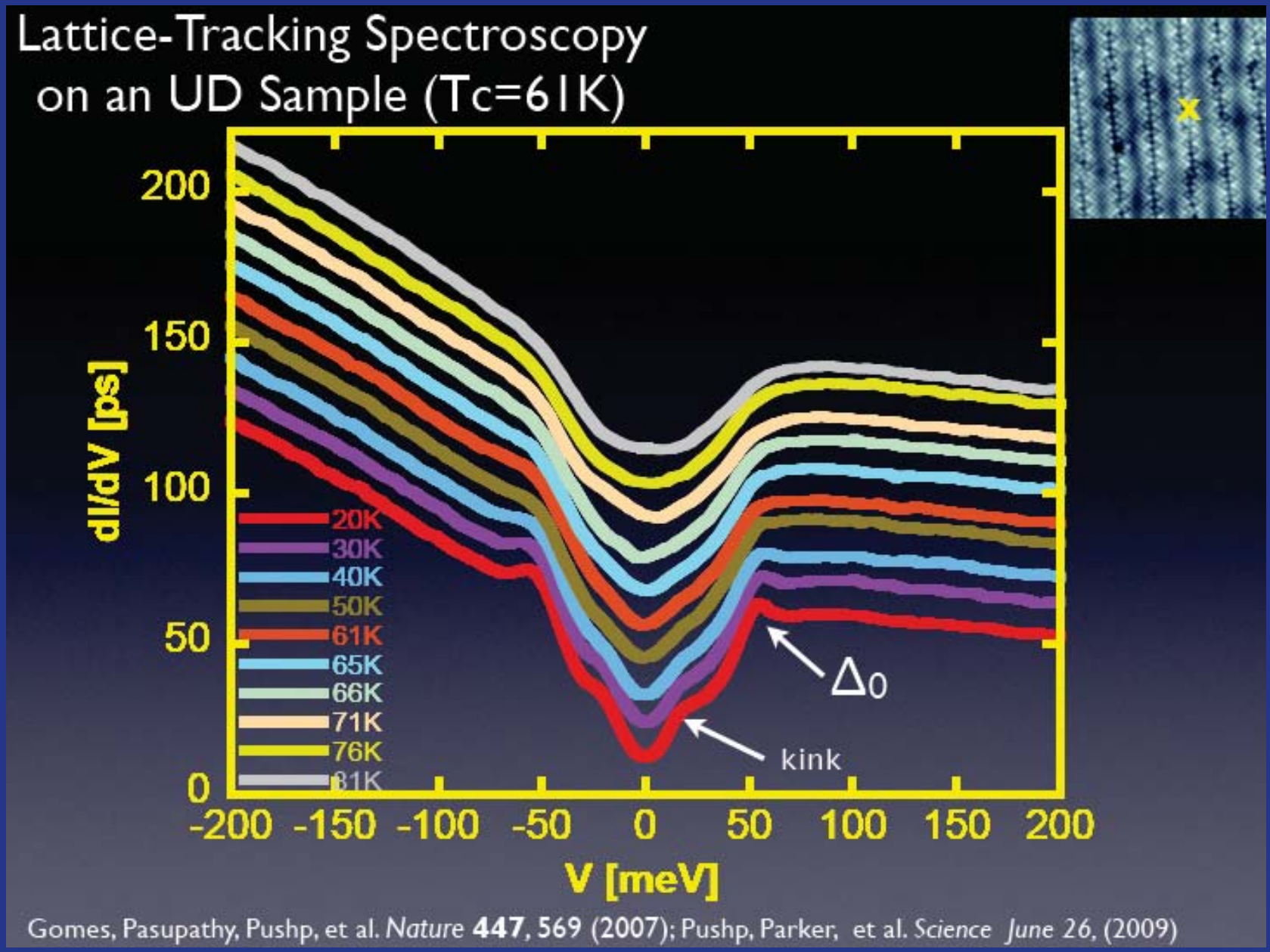

Courtesy Ali Yazdani, 2009

Why is this challenging for theory ?

- Approach to the Mott insulator: *quasiparticle coherence scale*
- Brinkman-Rice/Slave bosons/DMFT: *Uniform scale along Fermi surface (*of order δt)
- In constrast, in cuprates, *strong differentiation in momentum space is observed*
- Need to take into account inter-site superexchange (J)

→ singlet formation/antiferro spatial correlations

Some key questions…

- Is the pseudogap a precursor effect of pairing ?
- Does the PG state correspond to a broken symmetry (long-range order) setting in at T* ?
- Or is the PG rather a crossover due to the increasing tendancy to singlet formation as T is lowered ?
- Other mechanism (e.g. stripes) ?

- → Some of these questions will be adressed (if not answered in subsequent lectures and especially in seminars

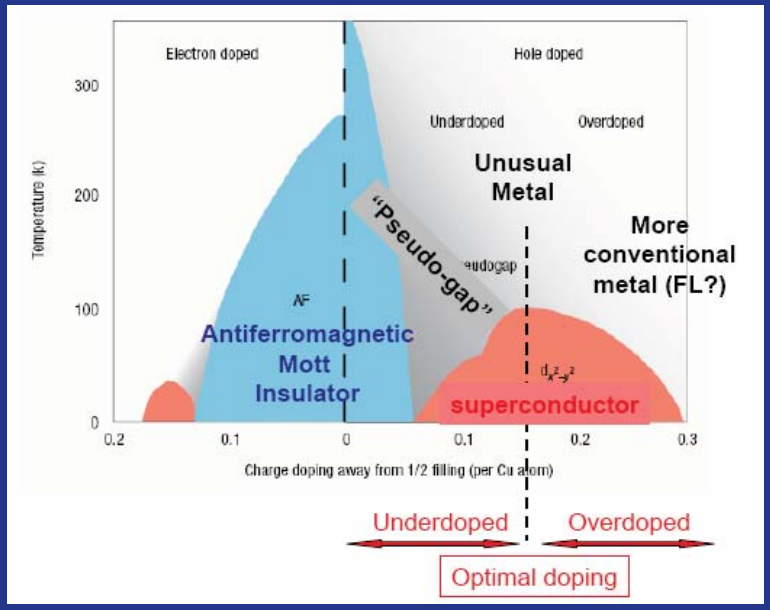

The `unconventional' metal: transport

Early transport data: Takagi et al. PRL 69 (1992) 2975

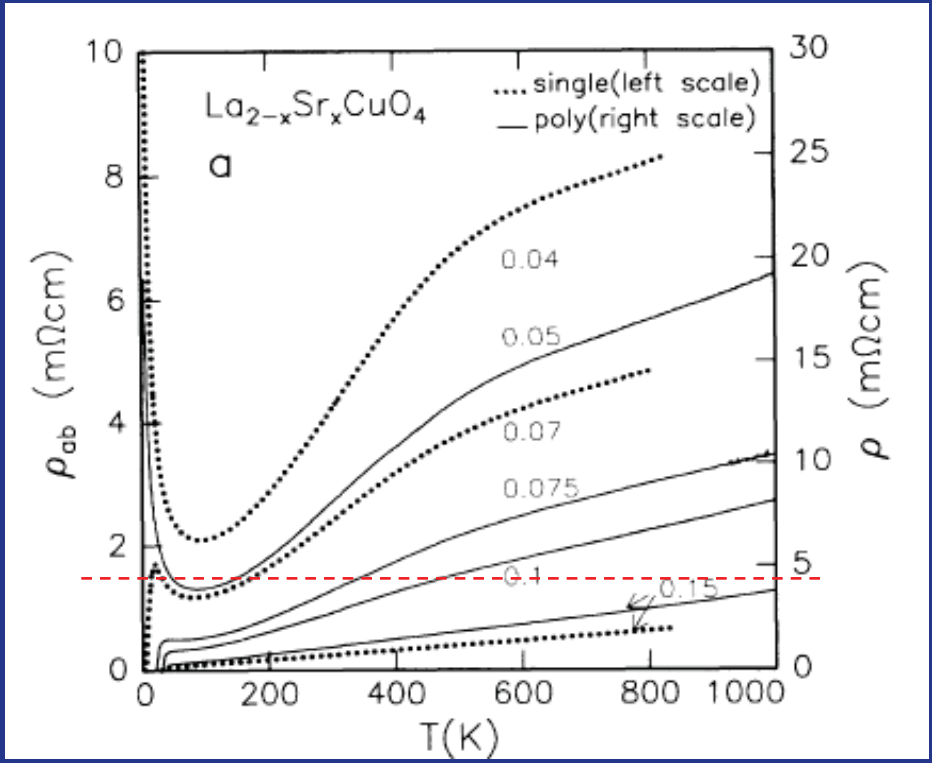

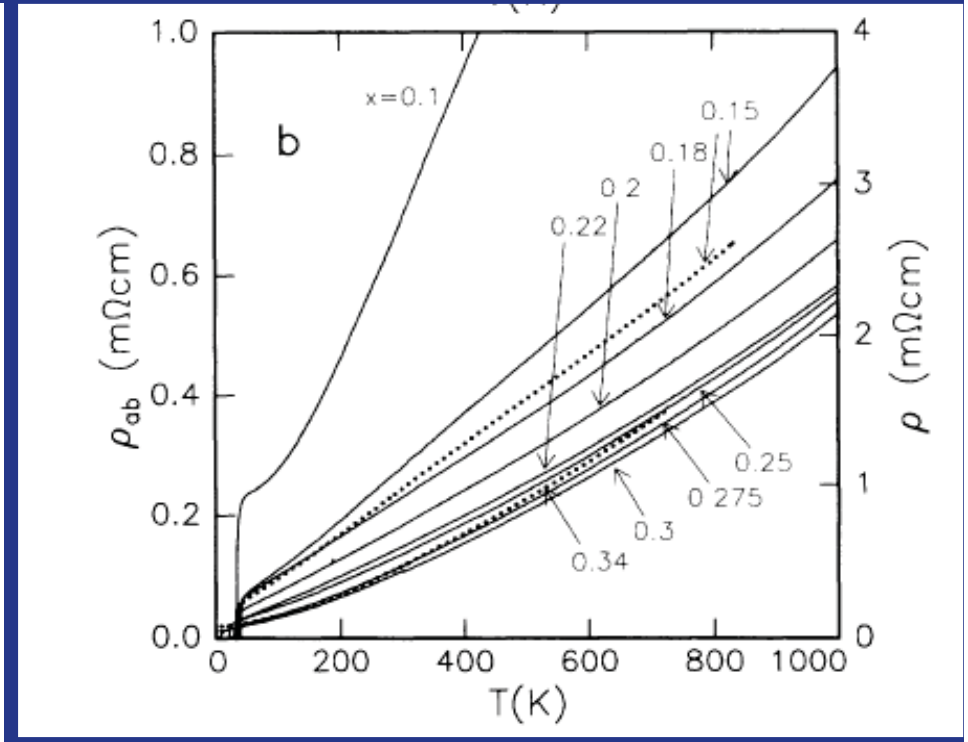

FIG. 1. The temperature dependence of the resistivity for $La_{2-x}Sr_xCuO_4$. (a) $0 < x \leq 0.15$, (b) $0.1 \leq x < 0.35$. Dotted lines, the in-plane resistivity (ρ_{ab}) of single-crystal films with (001) orientation; solid lines, the resistivity (ρ) of polycrystalline materials. Note, $\rho_M = (h/e^2)d = 1.7\ m\Omega\ cm$.

Underdoped → `bad metal' [Emery & Kivelson, PRL 74, 3253 (1995)]

Ioffe-Regel-Mott limit (quasi-2D case)

$$\sigma = \frac{ne^2\tau}{m^*}$$

$$l = v_F\tau \ , \ v_F = \frac{\hbar\tau}{m^*}$$

$$n = 2.\int_{FS}\frac{d^3k}{(2\pi)^3} \simeq 2.\frac{1}{8\pi^3}.\pi k_F^2.\frac{2\pi}{d}$$

d: interlayer distance

$$\rho = \rho_M\,(k_F l) \ , \ \rho_M = \frac{h}{e^2}\,d$$

Mott limit

$$\rho > \rho_M \rightarrow l < \lambda_F$$

Quasiparticle/Drude/Boltzmann description does not apply !

WARNING: this reasoning assumes a uniform scattering rate along large FS…

Summary of transport regimes: (slightly) different views based on different data analysis

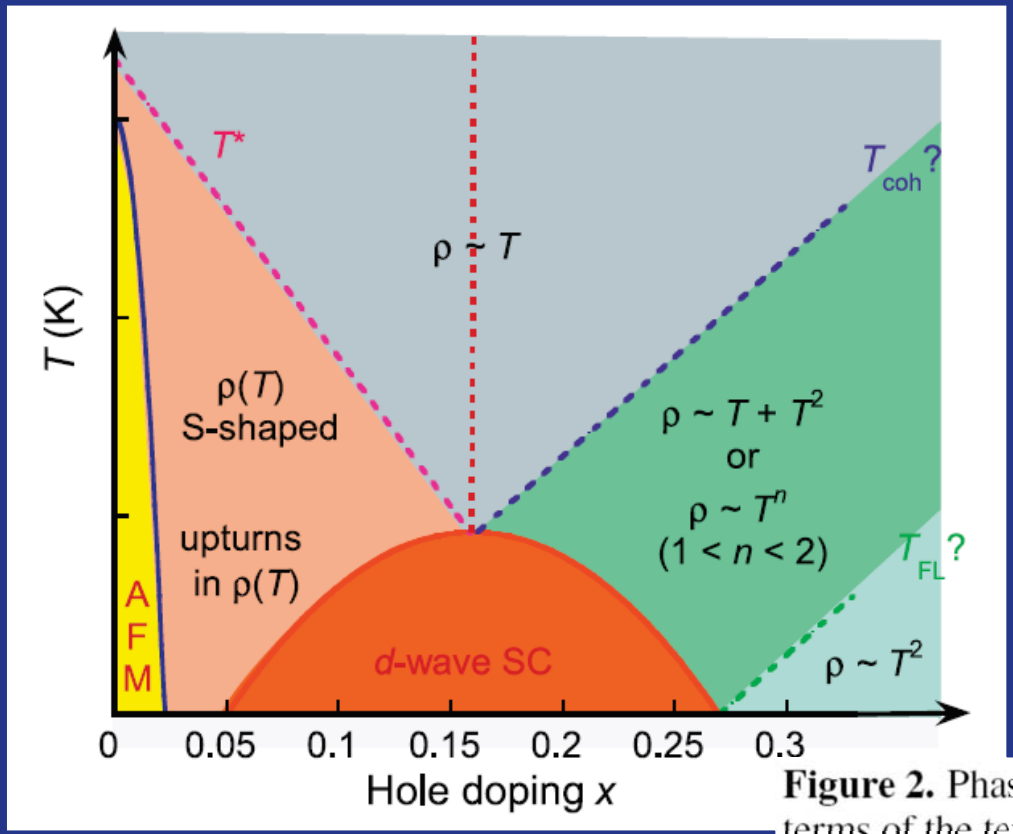

Recent review:
N.E.Hussey J.Phys
Condens Matter 20
(2008) 123201

(Hole-doped cuprates)

Figure 2. Phase diagram of (hole-doped) cuprates mapped out in terms of the temperature and doping evolution of the in-plane resistivity $\rho_{ab}(T)$. The solid lines are the phase boundaries between the normal state and the superconducting or antiferromagnetic ground state. The dashed lines indicate (ill defined) crossovers in $\rho_{ab}(T)$ behaviour. The meanings of the labels T^*, $T_{\rm coh}$ and $T_{\rm FL}$ are explained in the text.

PRL 93, 267001 (2004) PHYSICAL REVIEW LETTERS

Electronic Phase Diagram of High-T_c Cuprate Superconductors from a Mapping of the In-Plane Resistivity Curvature

Yoichi Ando,* Seiki Komiya, Kouji Segawa, S. Ono, and Y. Kurita

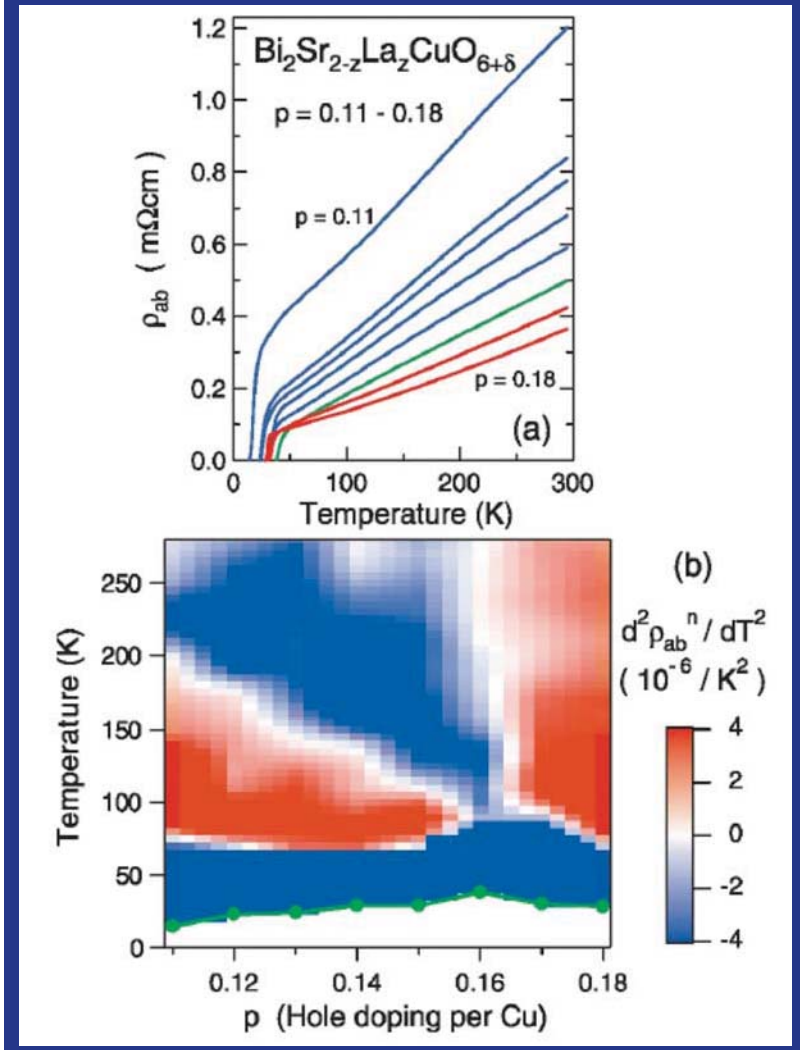

Ando et al:

- Strict linearity only very close to optimal doping ?
- PG crossover Identified from inflexion point

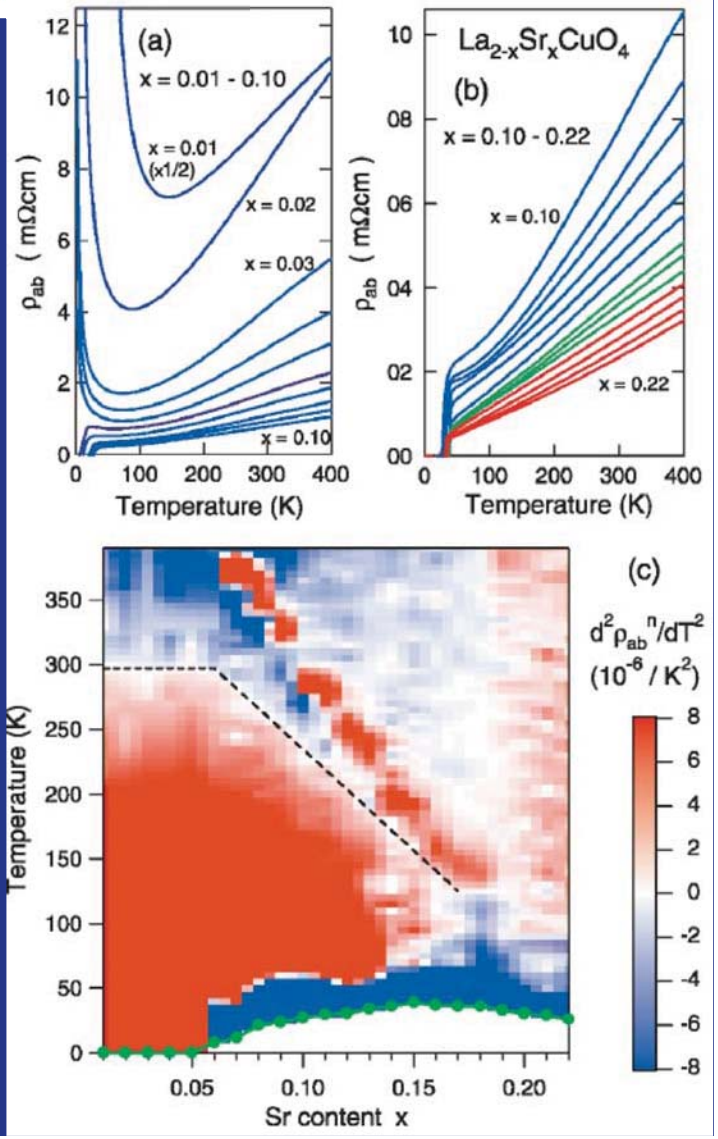

How should the T* scale be identified from transport measurements, and disentangled from SC fluctuation scale ?

Ando et al: inflexion point [Albenque et al. EPL 91, 37005 (2010)

However] this leads to a T* scale consistently lower (by roughly a factor of 2) than the NMR determination…

→ Need to look at a wider range of temperatures.

doping dependence qualitatively similar however

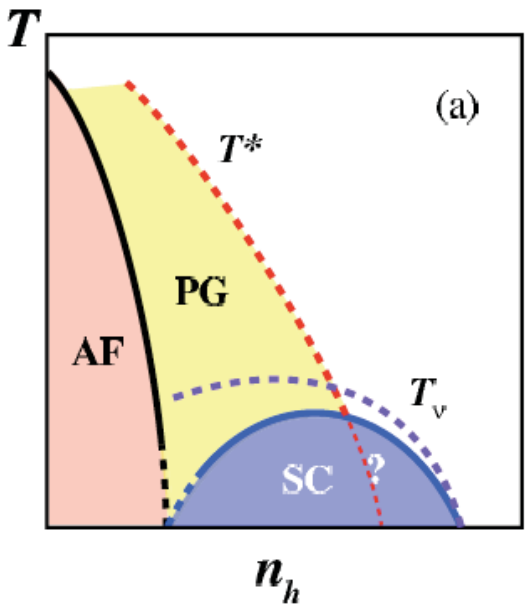

Clear distinction Between SC Fluctuation scale and PG scale

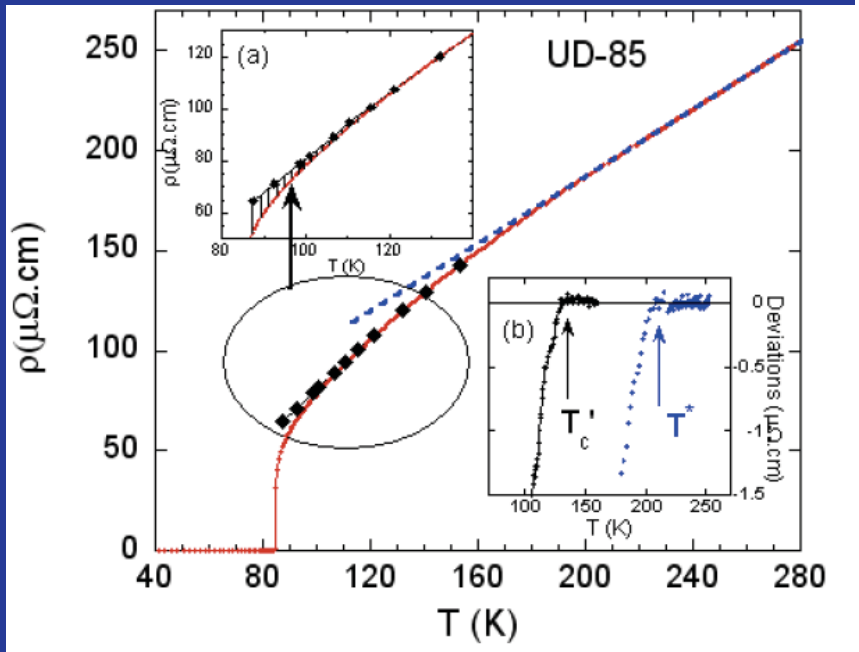

Linear resistivity:

- Is a universal hallmark of optimally doped samples
- In-plane resistivity per layer very similar between different materials (w/ vastly different anisotropies)

Table 1. ρ_{ab} (300 K), normalized ρ_{ab} (300 K) and ρ_c/ρ_{ab} (T_c) values for some optimally doped cuprates.

Compound	$\rho_\parallel$ ($T = 300$ K) ($\mu\Omega$ cm)	$\rho_\parallel$/layer (300 K) ($\mu\Omega$ cm)	$\rho_\perp/\rho_\parallel$ (T_c)
$YBa_2Cu_3O_{6.95}$	290 [39]	580	3×10^1 [40]
$La_{1.83}Sr_{0.17}CuO_4$	420 [39]	420	3×10^2 [41]
$Bi_2Sr_{1.61}La_{0.39}CuO_6$	500 [39]	500	1×10^6 [42]
$Bi_2Sr_2CaCu_2O_{8+\delta}$	280 [43]	560	1×10^5 [43]
$Tl_2Ba_2CuO_{6+\delta}$	450 [44]	450	2×10^3 [45]

Key points:

- Large non-saturating resistivity at low doping levels → ``bad metal'' (Emery-Kivelson PRL 1995)
- Linear-T dependence near optimal doping
- Approximate linearity above T* too
- Deviates from linearity at a scale ~ T* (actually > T* : gradual crossover) → loss of scattering (optics)
- Upturn at low-T at very low doping (impurity effect, cf. H.Alloul's seminar and Albenque et al EPL 81, 37008 (2008)
- Overdoped: much better metal, gradually more FL like
- Low-T behavior for SC samples ?

→ hi-magnetic field experiments

Downturn of resistivity at ~ T* can be interpreted as the loss of some inelastic scattering channel

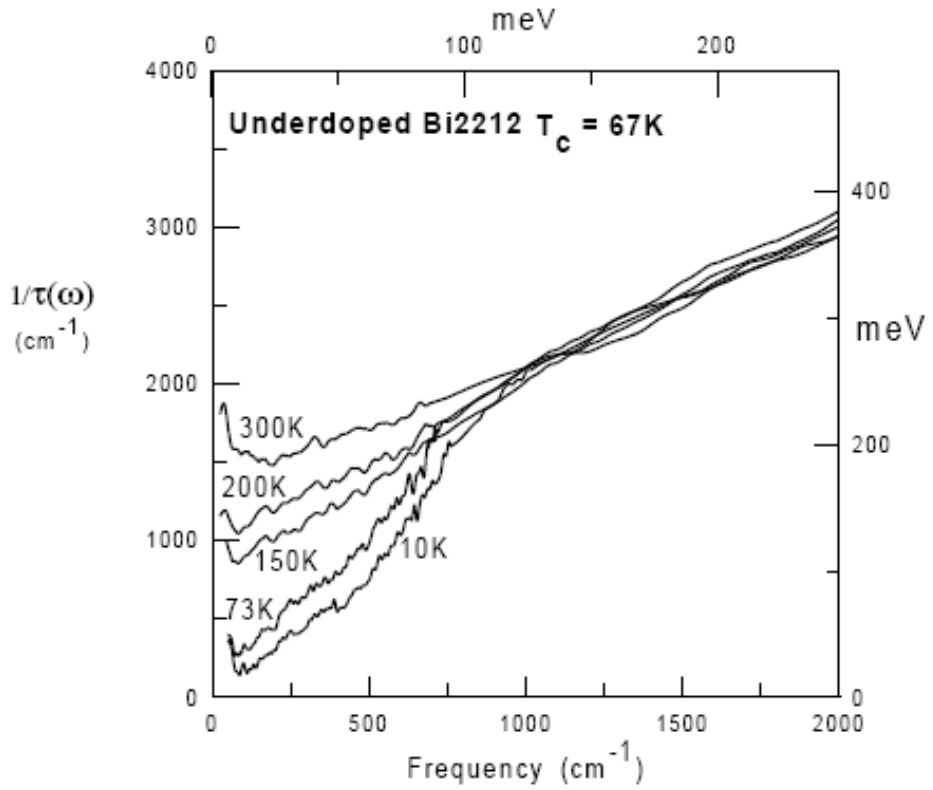

Figure 29. The frequency-dependent scattering rate and the effective mass of underdoped Bi 2212. The linear scattering rate develops a gap below 150 K. The frequency scale of this gap is only slightly enhanced in the superconducting state. There is no temperature dependence of the scattering at high frequency.

Optics

Transport/ some questions

- Need better understanding and theoretical handling of `bad metals'
- Origin of linear resistivity at opt. doping ?
- Is the scattering responsible for the linear resistivity at optimal doping also responsible for the hi-T resistivity above T* in the underdoped regime ?